EPJ D
Atomic, Molecular, Optical and Plasma Physics
EPJ.org
your physics journal

Eur. Phys. J. D (2013) 67: 191 DOI: 10.1140/epjd/e2013-40096-3

On some necessary conditions for p-^{11}B ignition in the hot spots of a plasma focus

Andrea Di Vita

edp sciences
Società Italiana di Fisica
Springer

Eur. Phys. J. D (2013) 67: 191
DOI: 10.1140/epjd/e2013-40096-3

THE EUROPEAN PHYSICAL JOURNAL D

Regular Article

On some necessary conditions for p-^{11}B ignition in the hot spots of a plasma focus

Andrea Di Vita[a]

DICCA, Università di Genova, Via Montallegro 1, 16145 Genova, Italy

Received 22 February 2013 / Received in final form 9 May 2013
Published online 25 September 2013 – © EDP Sciences, Società Italiana di Fisica, Springer-Verlag 2013

Abstract. Recently, it has been predicted that hydrogen-boron (p-^{11}B) nuclear fusion may attain ignition in the hot spots observed in a plasma focus (PF) pinch, due to their huge values of particle density, magnetic field and (reportedly) ion temperature. Accordingly, large magnetic fields should raise electronic Landau levels, thus reducing collisional exchange of energy from ion to electrons and Bremsstrahlung losses. Moreover, large particle densities, together with ion viscous heating, should allow fulfilment of Lawson criterion and provide effective screening of cyclotron radiation. We invoke both well-known, empirical scaling laws of PF physics, Connor-Taylor scaling laws, Poynting balance of electromagnetic energy and the balance of generalised helicity. We show that the evolution of PF hot spots is a succession of relaxed states, described by the double Beltrami solutions of Hall-MHD equations of motion. We obtain some necessary conditions for ignition, which are violated in most realistic conditions. Large electromagnetic fields in the hot spot accelerate electrons at supersonic velocities and trigger turbulence, which raises electric resistivity and Joule heating, thus spoiling further compression. Ignition is only possible if a significant fraction of the Bremsstrahlung-radiated power is reflected back into the plasma. Injection of angular momentum decreases the required reflection coefficient.

1 The problem

A plasma focus (PF) is a kind of pinch discharge in which a high-pulsed voltage is applied (with the help of a bank of capacitors with energy W_{cb}) to a low-pressure gas between coaxial cylindrical electrodes, generating a short-duration, high-density plasma region in the axis (see Ref. [1] for a comprehensive review). The pinch observed in front of the anode at the final stage of a well-behaved PF discharge [2] is made of a dense, hot plasma. Typical ranges for the electron density n_e, the electron temperature T_e, the ion temperature T_i and the amplitude B of the magnetic field $\mathbf{B}$ are $5 \times 10^{24} < n_e < 10^{26}$ m^{-3}, $0.1 < T_e < 2$ KeV, $0.3 < T_i < 1.5$ KeV (for a pure deuterium plasma) and 80 T $< B <$ 200 T, respectively [1].

A distinct feature of PF is scalability: smaller and larger PFs have basically the same dynamic characteristics, and the pinch energy density is practically the same for PFs in the range $50 \leqslant W_{cb} \leqslant 10^6$ J, once these machines are tuned for optimal operation (for a review of the relevant scaling laws, see Ref. [2]). In particular, if the working gas is pure deuterium, then the yield Y_n of DD fusion neutron per shot scales approximately as $Y_n \propto W_{cb}^2$. In the past, this scaling gave hopes of possible development as a fusion energy source. Conceptually, such source would have been much cheaper and simpler than those proposed by conventional approaches (either magnetic or inertial confinement) to controlled nuclear fusion [3]. Unfortunately, this favourable scaling deteriorates (down to $Y_n \propto W_{cb}^{0.8}$) at large W_{cb}. Many explanations have been proposed for this saturation [4,5], which has led to shut down of many fusion-focussed PF activities.

Analysis of X-ray emission shows that the internal structure of the pinch is made of well-defined filamentary structures [6,7] of radial size $\approx c/\omega_{pe}$ [8,9] (c light speed in vacuum, ω_{pe} electron plasma frequency), as well as of intensely radiating, small, short-lived macroscopic entities, called by various authors "hot spots" [10,11], "micropinches" [12–14], "plasmoids" [15] or "bright spots" [12,16]. We refer to these entities with the wording "hot spots" in the following. Structures resembling hot spots have been observed even at $W_{cb} = 50$ J [17]. Ranges for hot spot size a_{HS}, life-time τ_{HS}, electron temperature T_{eHS} and electron density n_{eHS} are 10 μm [11] $\leqslant a_{HS} \leqslant$ 300 μm [18], 0.5 ns [18] $\leqslant \tau_{HS} \leqslant$ 100 ns [19], 0.5 keV $\leqslant T_{eHS} \leqslant$ 5 keV [11,18] and 10^{26} m^{-3} [11] $\leqslant n_{eHS} \leqslant 10^{28}$ m^{-3} [20], respectively. Record values $\tau_{HS} = 1$ μs and $n_{eHS} = 10^{30}$ m^{-3} have been reported in reference [21] and reference [13], respectively; the former has been questioned in reference [20]. As for the amplitude B_{HS} of $\mathbf{B}$ inside a hot spot, preliminary, order-of-magnitude estimates give $B_{HS} \approx 10^5$ T [1]. Furthermore, simulations lead to a 1.8×10^4 T magnetic field near the core of pinched filament [22]. One experiment has been

[a] e-mail: anna_andrea.divita@tin.it

performed [23], in which the value $B_{HS} = 1.6 \times 10^4$ T was obtained. This is in qualitative agreement with the arguments of [24], according to which B_{HS} should be sufficiently strong to trap ions with energies ≈5 MeV/nucleon.

Within hot spots, huge values of n_{eHS} may lead to high rates of nuclear reactions, as these rates increase with increasing product of the densities of the reacting nuclei, which in turn scale with n_e for quasi-neutrality (see Refs. [18,24] and references therein). Admittedly, there is no general consensus about the relevance of hot spots to nuclear reactions. For example, according to [25] the neutron yield in PF deuterium discharges is not correlated to the number of pinch "necks" – roughly speaking, here by "neck" we mean "a narrow region of the plasma column" – which in turn have been correlated to hot spots [20]; moreover, the neutron emitting zone approximately coincides with the whole, dense plasma blob, which is much larger than the neck size. In contrast, according to [26] "all reaction yields and ion energy spectrum data" in PF discharges with deuterium and small quantities of CH_4, C_3D_8 or N_2 "are consistent with the view that the bulk of the reactions occur in a multiplicity of localized regions with a density of $>10^{26}$ m^{-3}"; moreover, "the bulk of DD fusion reactions occurs only inside hot spots", "the typical linear dimensions of a hot spot are smaller than the observed minimum diameter" of pinch necks, and "the number of hot spots [...] increases with Y_n". The authors of [26] claim also that insertion of suitable (and patented [27]) "field distortion elements (FDEs) into the interelectrode gap" raises "the number of hot spots where nuclear reactions take place in the pinch" so that multiplication of Y_n "by a factor of ⩾5" follows.

Of course, the rates of nuclear reactions may depend also on the energy E_{iHS} of the ions inside the hot spot, which in turn depends on the energy supplied to the hot spot by the external world (in the following, we replace E_{iHS} with the ion temperature T_{iHS} in the hot spot whenever a Maxwellian ion distribution is assumed). Both PF scalability and physical intuition would therefore suggest that E_{iHS} increases within increasing W_{cb}. However, according to [28–30], even if W_{cb} is as low as 50 kJ optimal energy transfer from the condenser bank to the hot spots occurs at relatively low external inductance (15 nH), small anode radius (2.8 cm) and large pressure of the working gas (10÷24 Torr). Here the word "relatively" means "with respect to the scaling laws described in reference [2] for optimization of Y_n in pure deuterium plasma". In an experiment with pure deuterium which satisfies these constraints, a value $E_{iHS} > 150$ KeV has been reported [31]. Results of reference [31] confirm previous results of the same group [29]. Further progress is predicted [30] if a weak (few Gauss), axial magnetic field is superimposed; the authors claim that such field should allow beneficial injection of angular momentum into the plasma. To the author's knowledge, however, no confirmation has yet been provided by independent researchers.

Ion energies above 150 KeV are relevant to the proton-boron (p-^{11}B) fusion reaction ($p + {}^{11}B \rightarrow 3\alpha + 8.6$ MeV), as its reaction reactivity (σv) reaches the maximum value for $T_i > 200$ KeV [32,33] for Maxwellian ion distribution. Lawson criterion for p-^{11}B ignition in PF hot spots reads [34]:

$$n_{eHS}\tau_{HS} \geqslant f\,(T_{iHS}, \varepsilon \ldots), \tag{1}$$

where ε is the fraction of boron density to proton density; below we take $\varepsilon = 0.09$, a value corresponding to maximum fusion power [22], and refer to n_i as to the proton density, so that the fusion rate $\propto n_i^2$. The detailed form of the function f on the R.H.S. is given by equation (14) of reference [34]. Remarkably, this equation seems to ignore both the recent amendments in the measured p-^{11}B cross section [35] and the resonance at 148 KeV [36]; however, it takes into account the "quantum suppression effect" (see below). The p-^{11}B reaction is of interest as it involves no radioactive material (like, e.g. tritium), releases no neutron (but those produced by the ensuing reaction ${}^{11}B + \alpha \rightarrow {}^{14}N + n + 157$ KeV, which carry less than 0.2% of the total energy released) and allows direct energy conversion from charged α's to electric power. Thus, should the results of reference [31] be confirmed, it would mean "a rebirth of the PF as a fusion energy device" [2].

The claims of reference [31] are far from unlikely. Two independent experimental results hint at the possible occurrence of energetic ions inside the hot spots in the PF pinch. Firstly, it has been reported that the pinch of a 25 kJ PF emits X photons with energy >30 KeV [37], in contrast to the hard X photons usually emitted by the anode surface when hit by energetic electrons coming from the pinch [38]. Secondly, the X photons emitted by hot spots are more energetic than the photons emitted by the remaining regions of the pinch in the experiments described in reference [39]. As for plasmas other than PF, a 20-fold increase in T_i – due to direct ion heating ruled by direct conversion of magnetic energy into ion thermal energy – has been reported in reconnection experiments [40].

More to the point, we recall that the plasma in reference [31] is pure deuterium, while heavier (boron) species are involved in p-^{11}B reaction. As for pinches with heavy ions, $T_i > 200$ KeV is reported in wire-array Z-pinch experiment at Sandia [41]. Rapid conversion of magnetic energy to a very high ion temperature plasma through the generation of fine scale, fast-growing $m = 0$ interchange magnetohydrodynamic (MHD) instabilities has been invoked. These instabilities saturate nonlinearly and provide ion viscous heating. Then, the ion energy is transferred to the electrons.

Per se, however, high ion energies are not enough for p-^{11}B ignition. Bremsstrahlung losses (which increase with increasing T_e) exceed fusion power already at $T_e = 200$ KeV [42]. In order to achieve ignition, we need therefore to keep T_e as low as possible, while maintaining ions at high temperature. Since electrons are heated by ions through collisions, the latter requirement implies that the collisional transfer of energy from ions to electrons is somehow controlled. Indeed, it has been shown that huge magnetic fields have favorable impact on Coulomb logarith [43]. Moreover, quantization of angular momentum implies that electrons in a magnetic field can have only discrete energy ("Landau") levels E_n (electron Larmor

radius cannot, e.g. be smaller than the De Broglie wavelength of the electron). The difference in energy between adjacent Landau levels is $\hbar\Omega_i$, where $\hbar$ and Ω_i are Planck's constant divided by 2π and the ion cyclotron frequency, respectively. Energy transfer from ions to electrons is reduced if [30]:

$$\frac{m_e}{m_i} E_{iHS} < \hbar\,\Omega_i \tag{2}$$

(m_i and m_e ion and electron mass, respectively), where we have neglected the electron motion parallel to $\mathbf{B}$ for large B. This "quantum suppression" effect [43] has been originally investigated in astrophysics [44,45] (something similar occurs in degenerate plasmas, where some transitions between electron states are forbidden [46]). For boron ions at 300 KeV, (2) requires $B > 1.3 \times 10^5$ T, i.e. less than one order of magnitude larger than the measured value in reference [23].

Inequality (2) is concerned with Bremsstrahlung. Another necessary condition is concerned about cyclotron radiation, which may induce strong radiation losses. Ignition is possible only if cyclotron radiation is effectively screened inside the hot spot, i.e. [28]:

$$2\omega_{pe} > \Omega_e \tag{3}$$

(Ω_e electron cyclotron frequency). Given B_{HS}, (3) provides us with a lower bound on n_{eHS}.

The above discussion justifies the suggestion of reference [34], which is based on the arguments of references [28–30] and is supported by independent simulations [22]: p-^{11}B ignition is possible in hot spots of the PF pinch through simultaneous ion viscous heating [41], quantum suppression [43] and cyclotron screening [28]. Further ion heating is due to interaction with beams of fast electrons born in the hot spots [30].

Accordingly, p-^{11}B ignition is the subject of a recent agreement between US and Iran research centers [47]. Improbable as it sounds, success depends critically on the predictions of references [29,30], as well-known scaling laws [2] scarcely apply here (see, e.g. figure 6 of Ref. [30]).

According to [30], the road to ignition is made of four steps. In the 1st step, the current sheath moving through the plasma between electrodes breaks up into an array of filaments [4]. The filamentary current sheath, driven by the interaction of its own currents and magnetic field, travels down to the end of the anode (in a time $t_{\rm pinch} \approx$ few μs), where the filaments converge into a single central pinch region. In the 2nd step, this pinch retains a filamentary structure [6]. Each filament has its own kinky shape and evolves "like an over-twisted phone cord" [30] until it is transformed into a hot spot (details are given below). In the 3rd step, the hot spot collapses somehow, until large values of density and magnetic field are reached [48]. In the 4th step, large electric fields are generated at the expense of the energy stored in the hot spot, and beams of charged particles are emitted [21].

The aim of this paper is to discuss the feasibility of this scenario. In the following, we refer to the value of the generic quantity a at the beginning of the 1st, the 2nd, the 3rd and the 4th step as to $a_{\rm working}$, $a_{\rm pinch}$, a_c, and a_{HS}, respectively, the final value of a at each step being the initial value at the following step. Our strategy is to compute the relevant a_{HS}'s as functions of the $a_{\rm working}$'s, and to use equations (1)–(3) in order to find those initial conditions $a_{\rm working}$'s (if any) which allow ignition.

As for the 1st step, we take $T_i = T_e$ for simplicity. Moreover, we are going to invoke the well-known scaling laws of reference [2] in order to obtain information concerning the $a_{\rm working}$'s. Admittedly, this approach is far from rigorous, as such scaling laws are just rule-of-thumb descriptions of PFs which are optimised for DD fusion and production of X-rays, not for p-^{11}B fusion. Lack of alternatives (few researchers, if any, ever investigated such p-^{11}B nuclear fusion in PFs) forces, therefore, our conclusions to be preliminary. However, an independent assessment of the predictions of references [30,34] (no matter how preliminary) is definitely no academic question, given the present concerns about delays and costs in magnetic- and inertial-confinement programs [49,50].

For each step we compute some physical quantities, including n_e and the generalised helicity $H \equiv \int \mathrm{d}\mathbf{x}\ \mathbf{V}\cdot\mathbf{\Omega}$, where $\mathbf{\Omega} = \nabla\times\mathbf{V}$, $\mathbf{B} = \nabla\times\mathbf{A}$ and $\mathbf{A}$, $\mathbf{V} = Ze\mathbf{B} + m_i\mathbf{v}$ and $e = 1.6\times10^{19}$ C are the vector potential, the conjugate momentum of an ion with ionisation number Z and the elementary charge respectively. As for n_e, quasi-neutrality ensures $n_e = Zn_i$ at all times, n_i ion particle density (we are interested in n_i as fusion rate $\propto n_i^2$). Since $\varepsilon = 0.09$, for our purposes it is reasonable to take $Z \approx 1$ in the following (actually, the averaged value Z for $\varepsilon = 0.09$ is 1.32). Accordingly, we write:

$$n_i \approx n_e \tag{4}$$

in all steps. As for the (usually overlooked) quantity H, we investigate it because it is an exact invariant of motion in dissipation-free Hall MHD [51], and Hall MHD is useful [48] in the description of both 2nd and 3rd step (see below); evolution of H is, therefore, likely to provide us with information about the impact of dissipation on the plasma structure.

We discuss the 1st step in Section 2. Filaments and hot spots share some common physics, which is discussed in Sections 3 and 4. We describe the 2nd, the 3rd and the 4th step in Sections 5–7, respectively. We compare the results with equations (1)–(3) in Section 8. Possible refinements are discussed in Section 9. Conclusions are drawn in Section 10. We are going to invoke some results of [48] again and again throughout the paper; this choice is justified in Section 6. Finally, we adopt SI units – but for temperatures, which are in eV.

2 The 1st step

Together with equation (4), the equation of state for perfect gases

$$\begin{aligned} p_{\rm working} &= (n_{i\,\rm working} + n_{e\,\rm working})\, e\, T_{\rm working} \\ &= 2\, n_{i\,\rm working} e\, T_{\rm working} \end{aligned} \tag{5}$$

the ion mass balance ($a_{\rm pinch}$, $a_{\rm working}$ pinch and anode radius, respectively)

$$n_{i\,\rm working}\pi\, a^2_{\rm working} = n_{i\,\rm pinch}\pi\, a^2_{\rm pinch} \tag{6}$$

and the following empirical scaling laws ($W_{\rm kin\,pinch} = \int_{\rm pinch} {\rm d}\mathbf{x}\, \frac{\rho\,|\mathbf{v}|^2}{2}$ kinetic energy in the pinch, $I_{\rm pinch}$ electric current flowing across the pinch):

$$I_{\rm pinch} \approx 7.7\times 10^5 a_{\rm working}\, p^{1/2}_{\rm working} \tag{7}$$

$$W_{cb} \approx 1.8\times 10^9 a^3_{\rm working} \tag{8}$$

$$a_{\rm working}\times p^{1/2}_{\rm working} \approx 6.8\times 10^{-3} W^{1/2}_{cb} \tag{9}$$

$$a_{\rm pinch} \approx 0.13 a_{\rm working} \tag{10}$$

$$W_{\rm kin\,pinch} \approx 0.17 W_{cb} \tag{11}$$

link the $a_{\rm pinch}$'s and the $a_{\rm working}$'s. As for (7)–(11) see table 3 and §3.2 of reference [2], figure 15 of reference [3], equation (15) of reference [52] and §12A of reference [53], respectively. Admittedly, numerical coefficients in equations (7) and (8) are affected by large incertitude due to considerable scattering of measurements. The impact of this incertitude on our result is assessed in Section 9. Remarkably, equations (7) and (9) lead to $\log_{10} I_{\rm pinch} \approx 3.7 + 0.5\log_{10} W_{cb}$; this agrees qualitatively with experiments as far as $W_{cb} < 300$ kJ; saturation occurs (and the factor 0.5 is to be replaced with 0.08) as $W_{cb} \gg 300$ kJ (see figure 3 of Ref. [5]). Direct inspection shows that such saturation does not invalidate our main conclusions below. Equations (4)–(10) give:

$$n_{\rm e\,pinch} \approx 1.3\times 10^{22} W^{1/3}_{cb}/T_{\rm working}, \tag{12}$$

i.e. $n_{\rm e\,pinch} \approx O\,(10^{25}\ {\rm m}^{-3})$ for $T_{\rm working} \approx 0.025$ eV (room temperature) and $W_{cb} \approx O\,(kJ)$, in agreement with [1]. According to (12), $n_{e\,\rm pinch}$ depends only weakly on W_{cb}: this result is in qualitative agreement with the discussion in §3.2 of reference [2].

As for H, we invoke the MHD equation of motion

$$\rho\frac{\partial\,\mathbf{v}}{\partial\, t} + \rho\,\mathbf{v}\cdot\nabla\,\mathbf{v} = -\nabla p + \mathbf{j}\times\mathbf{B} \tag{13}$$

where ρ, p, $\mathbf{j}$ and $\mathbf{v}$ are the mass density, the pressure, the electric current density and the velocity, respectively. We show in the Appendix that equation (13) leads to $H_{\rm working} = 0$ and to:

$$H_{\rm pinch} \approx \frac{2\ \mu_0\, e\ I_{\rm pinch} t_{\rm pinch} m_i W_{\rm kin\,pinch}}{\pi\, n_{i\,\rm pinch} m_e a^2_{\rm working}}, \tag{14}$$

where $\mu_0 = 4\pi\times 10^{-7}$ T A^{-1} m. We are going to invoke (11), (12) and (14) in the following. Finally, experiments show that quality of the radial focus pinch deteriorates [54] unless the magnetic Reynolds number is much smaller than one. We will discuss this point in detail below.

3 Physics in common to filaments and hot spots: Turner

The typical linear size $l_{\rm typical}$ of both filaments and hot spots is $< c/\omega_{pi}$ (ω_{pi} ion plasma frequency), so that conventional MHD is to be replaced with Hall MHD. Within the pinch, $\mathbf{j}$ is concentrated in filaments. As for the inner structure of each filament, we may safely assume that $\mathbf{j}$ is so large that magnetic self-interaction is much stronger than interaction with "external" currents, i.e. either the currents of other filaments inside the pinch or currents outside the pinch. This argument applies to hot spots too; indeed, this is true for most of the present discussion, and the relevance to either filaments or hot spots of the following results will be discussed below for each result separately.

We are going to show below that the evolution of filaments and hot spots can be viewed as a succession of steady states ($\partial/\partial t = 0$). Virial theorem of conventional MHD [55] states that no magnetically confined steady-state plasma exists without interaction with external currents. So, we may reasonably write:

$$\mathbf{j}\ \times\mathbf{B} = O\ (B\,due\,to\,external\,currents/B) \ll 1 \tag{15}$$

for the Lorenz force density $\mathbf{j}\wedge\mathbf{B}$ in steady state (it is the magnetic interaction among filaments which keeps together the pinch as a whole). Admittedly, the original proof of the virial theorem holds for inviscid plasmas only. However, viscous force vanishes for vanishing velocity, and would, therefore, just slow down the expansion of a plasma subject to non-zero Lorenz force due to internal fields only. It is, therefore, still reasonable to assume (15) even for steady states of viscous plasmas.

Moreover, failure of conventional MHD casts doubts on the relevance of equation (15) to our problem. However, equation (15) agrees with the suggestion of references [4,15,56,57] for hot spots and the PF pinch as a whole, respectively. Relationship (15) is satisfied, e.g. in the reversed field pinch ("RFP"), where dynamo counteracts magnetic diffusion [58] and the life time $t_{\rm lifetime} = l_{\rm typical}/v_{\rm typical}$ is much longer than both the resistive diffusion timescale $\mu_0\sigma_{/\!/} l^2_{\rm typical}$ and the time $t_{\rm Alfvèn} = l_{\rm typical}/c_A$ required by Alfvèn waves to travel across the system, so that:

$$Al \gg 1 \gg Re_m. \tag{16}$$

Here $Al \equiv c_A/v_{\rm typical}$, $Re_m \equiv \mu_0\sigma_{/\!/} l_{\rm typical} v_{\rm typical}$, $v_{\rm typical} \equiv l_{\rm typical}/t_{\rm lifetime}$, $\sigma_{/\!/}$ and c_A are the Alfvén number, the magnetic Reynolds number, a typical velocity, the parallel electric conductivity and the Alfvén speed, respectively. As for $l_{\rm typical}$, we take $l_{\rm typical} \approx$ filament radius a_{in} and $l_{\rm typical} \approx$ hot spot radius for filaments and hot spots respectively. In equation (16), the inequality $1 \ll Al = t_{\rm lifetime}/t_{\rm Alfvèn}$ allows us to describe both filaments and hot spots as long-lived structures, whose evolution is basically a succession of steady states – as for hot spots, see e.g. [19]. The inequality $1 \gg Re_m$ coincides with the condition of good quality pinching in

the 1st step [54], because Re_m is an integral of motion according to [28]; we will confirm the latter result in Section 4. Inequality $1 \gg Re_m$ implies also that the impact of Joule heating is far from negligible. Such result contradicts the postulate $B/n_e \approx$ const. of references [28–30] (should we replace "$\approx$" with "=" this postulate would reduce to "frozen-field" condition $Re_m \to \infty$ of ideal MHD [55]).

The role of viscosity is also far from negligible, as the Reynolds number $Re \equiv l_{\text{typical}} v_{\text{typical}}/\nu$ is <1, just like Re_m (here ν is the kinematic viscosity). In fact, according to the scenario outlined in reference [41] and invoked in reference [34], viscous heating is fed by MHD instabilities with wave number k and viscous Lundquist number L_μ, where

$$L_\mu \equiv \frac{2\,\rho\,\left(c_A^2 + c_S^2\right)^{\frac{1}{2}}}{\left(\mu_\perp + \mu_{/\!/}/3\right)\,k} \approx 2; \quad kl_{\text{typical}} \approx 10^2 \tag{17}$$

in a plasma with speed of sound c_s, $\beta = (Al \times Ma)^{-2}$, Mach number $Ma \equiv v_{\text{typical}}/c_s$, parallel viscosity $\mu_{/\!/}\,(\propto T_i^{5/2})$, perpendicular viscosity $\mu_\perp = \mu_{/\!/}/(1+\Lambda_i^2)$, ion Hall parameter $\Lambda_i \equiv \Omega_i \tau_{ii}$ and ion-ion collision time τ_{ii}. It is natural to identify $(\mu_\perp + \mu_{/\!/}/3)\,\rho^{-1}$ with ν. Equation (17) reduces therefore to $Re = 100 Al^{-1}\,(1+\beta)^{-1/2}$ and $Re < 1$ for sufficiently large Al. We are going to discuss both viscous and Joule heating in the following.

As for viscous heating, quasi-neutrality and (15) imply that electromagnetic force is negligible, at least on timescales $\gg 1/\omega_{pi}$ which rule ion oscillations in filaments made of hydrogen and boron [22]. The remaining forces of interest are the advective force ($\propto \mathbf{v}\cdot\nabla\mathbf{v}$) and the viscous force ($\propto \Delta v_{\text{typical}} \propto l_{\text{typical}}^{-2}$, neglected in equation (13) for large values of l_{typical} in the 1st step). Advective force is negligible in comparison with viscous force as $Re < 1$. Moreover, $\beta_c = 0.11$ [48] and $\beta_{HS} \approx O\,(1)$ in hot spots (see below); since $Al \gg 1$ it follows that $Ma \ll 1$, i.e. the evolution is basically incompressible. Now, incompressible, viscous, steady-state flows with negligible advective force correspond to a constrained minimum of the viscous heating power, the constraint being the conservation of mass – a result due to Kortweg and Helmholz (see §327 of Ref. [59]).

As for Joule heating, it is ruled by Ohm's law. Some simplifications are possible. Firstly, according to [41] the contribution of magnetic fluctuations to Ohm's law is $\propto (kl_{\text{typical}})^{-1} \ll 1$, and we neglect it. Secondly, (15) allows us to neglect the contribution to the Joule heating power density P_J of the component of $\mathbf{j}$ which is perpendicular to $\mathbf{B}$. Thirdly, we assume (conservatively, for the assessment of fusion feasibility) that the energy transport is so effective that we may neglect ∇T_e. Then, the corresponding contribution of the thermal force to Ohm's law is also negligible. Moreover, in this case equation (5) of [41] implies $\nabla T_i = 0$, which is a conservative assumption as far as fusion feasibility is to be assessed. Fourthly, electrons rule electric conduction, i.e. the electric conductivity $\sigma_{/\!/}$ depends on T_e; then, we neglect $\nabla\sigma_{/\!/}$. Finally, we neglect the contribution of $\mathbf{v}\times\mathbf{B}$ to Ohm's law in comparison with the contribution of $1/\sigma_{/\!/}$, because $Re_m \ll 1$. In this case, it is shown in reference [48] that the total Ohmic heating power $P_\Omega \equiv \int_V d\mathbf{x}\, P_j$ in a region V of plasma is $P_\Omega = \int_V d\mathbf{x}\,\sigma_{/\!/}^{-1}\,|\,\mathbf{j}\,|^2$. This is in agreement with [60], where it is shown that magnetic fluctuations leave the total Joule power unaffected. Moreover, it can be shown that the steady state corresponds to a constrained minimum of Joule heating power, the constraint being provided by the conservation of electric charge – a result due to Kirchoff (see Refs. [61,62] and Problem 3 §21 of Ref. [63]).

Since the evolution of filaments and hot spots is just a succession of steady states where both Kortweg-Helmholz and Kirchoff's principles hold simultaneously, we conclude that filaments and hot spots corresponds at any time to a minimum of total dissipated (viscous + Joule) power. The same result had been obtained in reference [48], but starting from the assumption of local thermodynamic equilibrium (LTE), which is not relevant to the case $T_i \gg T_e$ we are to discuss here.

Regardless of LTE, three results are also derived in Sections 5 and 6 of reference [48]. Firstly, the following expressions:

$$\begin{aligned} \nabla\wedge\mathbf{v} &= r\,\mathbf{v} + w\,\mathbf{B} \\ \nabla\wedge\mathbf{B} &= l\,\mathbf{v} + g\,\mathbf{B} \end{aligned} \tag{18}$$

for $\mathbf{v}$ and $\mathbf{B}$ describe steady state solutions of the equations of motion which minimise the total dissipated power, in the limit of negligible ∇T_e and negligible interaction with external currents (r, w, l, g constant coefficients; their exact meaning is not relevant in the following).

Secondly, in the latter limit relationships (18) agree with (15).

Thirdly, (18) are the Euler-Lagrange equations of a variational principle which reduces to constrained minimisation of total (magnetic + kinetic) energy E_{TOT} with given magnetic helicity $K \equiv \int d\mathbf{x}\;\mathbf{A}\cdot\mathbf{B}$ and given generalised helicity H. The latter principle has been proposed by Turner [51] as a generalisation to Hall MHD of Taylor's minimisation of magnetic energy $W_{\text{magn}} \equiv \int d\mathbf{x}\,|\mathbf{B}|^2/(2\mu_0)$ with the constraint of given K [64]; solutions of Taylor's variational principle ("Taylor's states") satisfy the equation

$$\nabla\wedge\mathbf{B} = \lambda\,\mathbf{B} \tag{19}$$

with $\nabla\lambda = 0$ and $\lambda = K^{-1}\int d\mathbf{x}\,|\mathbf{B}|^2$, hence $\mathbf{j}\wedge\mathbf{B} = 0$ exactly.

Remarkably, Taylor's model, which originally aimed at description of relaxed states in MHD, is based on the "selective decay" approach [65]. This approach implies that one of the constants of motion of the ideal limit (here, W_{magn}) decays faster than the others (here, K). In the past, indeed, it has been proposed that a hot spot is in a three-dimensional (3D), toroidal [19] Taylor's state [15] similar to a spheromak [66]; moreover, Taylor's states have been invoked also for the PF pinch as a whole [56,57]. Admittedly, the relationship with Turner's principle could be a weak point of (18): in fact, Turner's principle has been objected [67,68] on the basis that H is not as well conserved as K, i.e. Turner's principle is in contrast with

selective decay. Nevertheless, Turner's theory has been invoked in order to describe hot spots [69]: it turns out that a hot spot corresponds simultaneously to a fluid vortex, a quasi-force-free magnetic field and a confined finite-pressure plasma which is able to trap energetic ions, just as suggested in reference [20] and claimed in reference [31]. We take these conclusions as an independent confirmation of the relevance of equation (18) to our discussion.

4 Physics in common to filaments and hot spots: CVHBS

The relevance of dissipative mechanisms like viscous and Joule heating prevents us from neglecting collisions. In order to take the latter into account, Nardi [19] applied kinetic equations to the description of toroidal, large-density hot-spots in the PF. Even the simplest kinetic (Vlasov) equation, which takes no collision into account, may lead to double Beltrami equilibria [70]. When discussing collisions, we invoke the findings of Connor and Taylor [71] and recall that the Collisional Vlasov High Beta Scaling (CVHBS) – namely, a set of scaling transformations for space, time and magnetic field – is the only scaling which allows invariance of the kinetic equation of collisional plasmas under the transformation $\mathbf{x} \to k\mathbf{x}$, k const. CVHBS includes:

$$\mathbf{x} \to k\,\mathbf{x}; \quad t \to k^{\frac{5}{4}} t; \quad \mathbf{B} \to k^{-\frac{5}{4}}\mathbf{B}. \tag{20}$$

It follows that $n_e \propto |\mathbf{x}|^{-D} \to k^{-D} n_e$ in the D-dimensional case ($D = 2$ for filaments, $= 3$ for hot spots), $\mathbf{v} \propto \mathbf{x}/t \to k^{-1/4}\mathbf{v}$, $\mathbf{E} \propto \mathbf{v} \wedge \mathbf{B} \to k^{-3/2}\mathbf{E}$, $\mathbf{j} \propto \nabla \wedge \mathbf{B} \propto$ (magnetic field)/(length) $\to k^{-9/4}\mathbf{j}$, $\sigma_{/\!/} \propto$ (electric current density)/(electric field) $\to k^{-3/4}\sigma_{/\!/}$, $P_\Omega \to k^{D-15/4} P_\Omega$, $K \to k^{D-3/2} K$, $H \to k^{D-3/2} H$ and $T_e \propto \sigma_{/\!/}^{2/3} \to k^{-1/2} T_e$. The latter result follows from the scaling $T_e \propto \sigma_{/\!/}^{2/3}$, which holds in both hot spots and filaments. As for hot spots, we invoke equation (10) of reference [21]. As for filaments, it is usually assumed that the electron drift velocity $V_d > c_s$ [28], so that:

$$\sigma_{/\!/} = \alpha\, 1.92 \times 10^4\, (\ln \Lambda)^{-1}\, T_e^{3/2} \tag{21}$$

where $\ln\Lambda$ and $\alpha \leqslant 1$ are the Coulomb logarithm for electron-ion collisions and a dimensionless factor which accounts for turbulence, respectively [72] (the case $\alpha = 1$ corresponds to Spitzer's law). Equation (21) seems to be a reasonable assumption, at least provided that the line-averaged electron density of the PF pinch does not exceed 10^{21} m^{-1} (see §11.1 of Ref. [1]).

Moreover, CVHBS leads to Re_m = const., in agreement with [28], as anticipated. Furthermore, CVHBS leads also to $|\mathbf{B}|\,(\text{radius})^{5/4}$ = const., a result invoked in order to extrapolate tokamak performances [73]. Finally, CVHBS gives $\beta \to k^{2-D}\beta$, a result we invoke below to compute β_{HS}.

5 The 2nd step

In the following we are going to link n_{ec}, T_{ec} and H_c with $n_{e\,\text{pinch}}$, $T_{e\,\text{pinch}}$ and H_{pinch}, respectively. Let N_f filaments, each with radius a_c, fill a pinch with radius a_{pinch}. Then, we may write $N_f \pi a_c^2 = \pi a_{\text{pinch}}^2$. According to Sections 11 and 12 of reference [48], N_f and the electron density n_{ec} satisfy the relationships $N_f = (a_{\text{pinch}}\omega_{pe\,\text{pinch}}/c)^2$ and $n_{ec} a_c^2 = \gamma\iota(2\pi r_e)$, respectively, where γ is the ratio of total energy of an electron to the rest mass energy $m_e c^2$ of an electron, $\iota \equiv I_c/I_{\text{Alfvèn}}$, I_c is the electric current flowing across a filament, $I_{\text{Alfvèn}}$ is the Alfvén-Lawson current, and $r_e \equiv \mu_0 e^2/(4\pi m_e)$ is the classical electron radius. It follows that:

$$n_{ec} = (2\gamma\iota) n_{e\,\text{pinch}}, \tag{22}$$

where $\omega_{pe} \equiv e n_e^{1/2}/(\varepsilon_0 m_e)^{1/2}$, $\varepsilon_0 = 8.85 \times 10^{-12}$ F/m. As for n_i, quasi-neutrality leads to a similar result. Furthermore, CVHBS for $D = 2$ gives β_c = const. (=0.11 [48]), $n_{ec} = (k_c/k_{\text{pinch}})^{-2} n_{e\,\text{pinch}}$ and $H_c = (k_c/k_{\text{pinch}})^{1/2} H_{\text{pinch}}$, so that (22) gives $k_c/k_{\text{pinch}} = (2\gamma\iota)^{-1/2}$ and:

$$H_c = (2\gamma\iota)^{-1/4} H_{\text{pinch}}. \tag{23}$$

(The actual values of k_{pinch} and k_c are not relevant here.) Typical values for γ and ι are [48]:

$$\gamma \approx 1; \qquad \iota \approx 5.2. \tag{24}$$

Together, (22) and (24) suggest that at the beginning of its life-time the hot spot particle density is ≈10 times the corresponding pinch value. Unpublished simulations seem to confirm this result [74].

6 The 3rd step

Experimental results are consistent with a model of radiative compression which explains the formation of hot spots as a result of both the onset of $m = 0$ instabilities [75] and of intense radiative losses via line emission by multiply charged heavy ions. Radiative cooling [20] is likely to be responsible for the increase in n_e in neon-seeded deuterium plasma discharges [1]. The addition of small amount of high-Z impurities helps the onset of radiation collapse [20,76] and may trigger the formation of hot spots [13,76,77]. It is therefore natural to assume that the collapse drives pinch filaments [7] into hot spots as n_e increases. Whatever the physical mechanism responsible for the collapse, the latter reduces l_{typical}; since both mass conservation and CVHBS imply $n_e \propto l_{\text{typical}}^{-D}$, according to (4) it is in the $D = 3$, hot spot configuration that the collapse is more likely to drive the plasma up to fusion-relevant values of n_i. Our conclusion agrees with the scenario outlined in reference [30], where ignition occurs at the very end of hot spot life. Accordingly, we have neglected the role of ion viscous heating in the previous steps.

Indeed, it has been shown [48] that solutions of (18) in PF are either filamentary and two dimensional ($D = 2$),

or spheromak-like, three-dimensional ($D = 3$) Taylor's states, depending on the value of n_e. If n_e exceeds a threshold n_{ec}, (i.e., if ω_{pe} exceeds a threshold ω_{pec}) then the plasma switches from structures with $D = 2$ to structures with $D = 3$, as it looks for the less dissipating configuration. The threshold is investigated in reference [78], where the results of independent numerical estimates on RFP are retrieved. Together with equation (19), equations (2.6) and (2.7) of reference [78] provide us with the threshold:

$$\omega_{pe} > \omega_{pec} = (0.3)\max\left(1,\ \Lambda_i\right) c\lambda. \tag{25}$$

Two independent confirmations of equation (25) are available. Firstly, the fact that the plasma switches from 2D- to 3D-collapse once a threshold is trespassed agrees qualitatively with the fact that timescale of hot spot formation is very short (<ns) (see Ref. [19] and figure 6c of Ref. [21]). Secondly, comparison of our equations (18) and equations (3) of reference [79] shows that the former include the well-known "double Beltrami" equilibria of Hall MHD [80] as particular cases. (Even addition of dust on PF pinch axis, which seems to be a promising path towards optimization of PF performances [81], still allows relaxation to states similar to double Beltrami equilibria where dynamo occurs [82] just like in states described by Taylor's principle [58]. However, in the following we focus our attention on dust-free PF plasmas, for simplicity.) Double Beltrami states are investigated in the physics of solar corona [79,80]. It turns out that abrupt transition to Taylor states described by equation (19) occurs when $\lambda \approx E_{TOT}/(2K)$ [83] becomes smaller [84] than a typical inverse length $\propto \omega_{pi}/c$, in qualitative agreement with (25). Similarity between PF and space plasma physics, respectively, is due to the validity of Hall MHD in both systems, and seems to support past analogies between them [15,28].

We have still to justify our utilisation of the results of reference [48]. To this purpose, we apply both CVHBS and Poynting balance of electromagnetic energy:

$$\nabla\left(\frac{\mathbf{E}\times\mathbf{B}}{\mu_0}\right) + \frac{\partial}{\partial\, t}\left(\frac{\varepsilon_0\left|\mathbf{E}\right|^2}{2} + \frac{\left|\mathbf{B}\right|^2}{2\,\mu_0}\right) + \mathbf{E}\cdot\mathbf{j} = 0 \tag{26}$$

to a spheromak with volume $V_S(t)$ collapsing radially at velocity $v_r(t)$. Remarkably, equation (26) contains T_i nowhere, hence its predictions depend on no particular ion heating mechanism. Ohm's law allows us to estimate the volume integrals of each term of equation (26) on V_S:

$$\int_{V_S} d\mathbf{x}\,\nabla\left(\frac{\mathbf{E}\times\mathbf{B}}{\mu_0}\right) = \frac{4\pi a_c^2 v_{r\,0} B_{*_c}^2}{\mu_0} k_*^{-\frac{3}{4}} \tag{27}$$

$$\int_{V_S} d\mathbf{x}\,\frac{\partial}{\partial\, t}\left(\frac{\varepsilon_0\left|\mathbf{E}\right|^2}{2} + \frac{\left|\mathbf{B}\right|^2}{2\,\mu_0}\right) = \frac{c_1 a_c^3 B_{*_c}^2}{2\mu_0}\frac{d}{d\,t}\left(k_c^{\frac{1}{2}}\right) \tag{28}$$

$$\int_{V_S} d\mathbf{x}\,\mathbf{E}\cdot\mathbf{j} = \frac{\sigma_{/\!/\,c} a_c^3 c_0 E_{*_c}^2}{\mu_0} k_c^{-\frac{3}{4}} \tag{29}$$

in the center-of-mass frame of reference (so that $\partial/\partial t = d/dt$), where we have introduced the quantities

$$k_* \equiv k/k_c, \quad E_* \equiv \max_{V_S}\left|\mathbf{E}\right|, \quad B_* \equiv \max_{V_S}\left|\mathbf{B}\right|,$$

$$c_0 \equiv a_c^{-3} E_{*_c}^{-2}\int_{V_{Sc}} d\mathbf{x}\,\left|\mathbf{E}\right|^2, \quad c_1 \equiv a_c^{-3} B_{*_c}^{-2}\int_{V_{Sc}} d\mathbf{x}\,\left|\mathbf{B}\right|^2$$

and we have neglected the contributions of both $\mathbf{j}\times\mathbf{B}$, ∇T_e and fluctuations to Ohm's law. Equations (26)–(29) lead straightforwardly to the equation for $k_*(t)$:

$$\frac{d}{d\,\tau_*}\left(k_*^{\frac{1}{2}}\right) + k_*^{-\frac{3}{4}} = 0 \tag{30}$$

with the dimensionless variable

$$\tau_* \equiv t\frac{v_{r\,c}}{a_c}\frac{8\pi}{c_1}\left[1 + \frac{c_0}{4\pi}\left(\frac{E_{*_c}}{v_{r\,c}B_{*_c}}\right)^2 Re_m\right],$$

$$Re_m = \mu_0 v_{rc}\sigma_{/\!/\,c} a_c.$$

(We recall that Re_m is a constant $\ll 1$.) The solution of equation (30) with the initial condition $k_* = 1$ is

$$k_* = \left(1 - \frac{5}{2}\tau_*\right)^{\frac{4}{5}}. \tag{31}$$

According to equation (31) and to CVHBS for $D = 3$, $P_\Omega \propto k_*^{-3/4}$ diverges only near the very end of the hot spot collapse, i.e. for $\tau_* \to 2/5$ (a similar result holds for viscous heating too). So, even if dissipation allows relaxation to Turner-like configurations at all times, we are allowed to neglect dissipation in the 3rd step (heating is taken into account in the following). Here, the main role of dissipation is just to ensure relaxation to double Beltrami states at all times during the collapse.

Section 12 of reference [48] provides us with a CVHBS-based description of collapsing Double Beltrami states under the assumption of $Z = 1$ and negligible heating. As for n_e, this description gives $n_{eHS} = 21\zeta^4 n_{in}$, where $\zeta \equiv eV_p/T_{ec}(J) = V_p/T_{ec}$, V_p is the peak electric voltage (in Volt) and n_{in} is the value of n_e in the 2D filament at the beginning of the collapse. Both T_{ec} and Φ are estimated below. As the collapse raises n_e while leading to a 3D structure, $n_{in} \leqslant n_{ec}$; since we are interested in the maximum attainable particle density in order to maximise the fusion rate, here and below we take for n_{eHS} its maximum allowable value:

$$n_{eHS} \approx 21\zeta^4 n_{ec}. \tag{32}$$

As for H, (32) and CVHBS for $D = 3$ give

$$n_{eHS} = (k_{HS}/k_c)^{-3} n_{ec} \quad \text{and} \quad H_{HS} = (k_{HS}/k_c)^{3/2} H_c,$$

hence:

$$H_{HS} \approx 0.22\zeta^{-2} H_c. \tag{33}$$

As for β, CVHBS for $D = 3$ gives $\beta_{HS}/\beta_c = (k_{HS}/k_c)^{-1} = (21)^{1/3}\zeta^{4/3}$ so that $\beta_{HS} \approx O(1)$ in most cases, as anticipated, provided that we neglect anomalous ion heating

due to viscosity. The actual value of β_{HS}/β_c depends on ion heating and is discussed below; in all cases, $Ma \ll 1$ even if $\beta_{HS} > 1$ provided that Al is sufficiently large. Finally, CVHBS leads to the following useful relationships [48]:

$$a_{HS} \approx 2.3 \times 10^7 \zeta^{-2} n_{ec}^{-1/2} \quad (34)$$

$$B_{HS} \approx 1.9 \times 10^{-12} \zeta^{5/2} n_{ec}^{1/2} T_{ec}^{1/2} \quad (35)$$

$$T_{eHS} \approx 0.14 V_p. \quad (36)$$

We are going to give an independent, approximate confirmation of equation (36) in the following.

7 The 4th step

So far, we have said nothing about the end of the collapse. Experimentally, it has been observed that the hot spot at its very end emits beams of electrons [11,85]. The latter carry away an enthalpy flux $\frac{5}{2} n_{eHS}\, e T_{eHS} V_{dHSz}$ in the axial direction, where $V_{dHSz} = j_z/(e\, n_{eHS})$, $j_z = \sigma_{/\!/} E_z$, $E_z = -d\Phi/dz$ and Φ are the axial component of the electron drift speed in the hot spot, the axial current density, the axial electric field and the potential which accelerates the electron beam emitted by the dying hot spot, respectively. For the moment, let us neglect the impact of dissipation, which we have shown to be small; we take it into account below. Then, the energy balance of the hot spot at the end of the collapse reads [21]:

$$j_z E_z = \frac{d}{d\, z}\left(\frac{5}{2} n_{eHS}\, e T_{eHS}\, v_{ezHS}\right). \quad (37)$$

Quasi-neutrality and Poisson's equation imply $dE_z/dz = 0$. Equations (21) and (37) lead therefore to $\frac{d}{dz}(T_{eHS} - \frac{4}{25}\Phi) = 0$ regardless of α. The boundary condition is $\Phi(T_{eHS} = 0) = 0$, as no electron energization occurs for zero hot spot energy. Then, (36) solves (37) approximately, provided that

$$\Phi \approx V_{\rm p}. \quad (38)$$

Such agreement provides further confirmation to CVHBS and is far from surprising for three reasons: (a) the model of reference [21] takes into account the voltage drop across just one hot spot; (b) the collapse is much faster than the typical voltage decay time $|V_p/dV_p/dt|$; (c) the proofs of both (36) and (37) rely on the assumption of negligible heating. However, as for the p-^{11}B ignition relationship (38) is still a quite optimistic assumption, since in real life V_p is just an upper bound on Φ. Accordingly, in the following we retain (38) as for the order of magnitude, but invoke no scaling law concerning V_p explicitly: we rather try to compute the maximum attainable value of Φ starting from the $a_{\rm working}$'s, as we are interested in necessary conditions for ignition. Reasonably, we expect such conditions to be affected by the insofar neglected dissipation.

In order to take Joule dissipation explicitly into account, we write down an order-of-magnitude estimate. To thus purpose, we follow [21] and describe the hot spot as a small cylinder of length l_{HS} and cross section S_{HS}, with $l_{HS} = 2a_{HS}$ and $S_{HS} = \pi a_{HS}^2$ in order to retain the meaning of a_{HS} as "hot spot radius". Ohm's law leads to $|\,\mathbf{j}| = \sigma_{/\!/}|\mathbf{E}|$, where we take into account the component of $\mathbf{j}$ parallel to $\mathbf{E}$ only as the hot spot is supposed to be a force-free structure. Typical values of $|\mathbf{E}|$ and $|\mathbf{j}|$ are Φ/l_{HS} and I_{HS}/S_{HS} where I_{HS} is the typical value of electric current in the hot spot. In order to estimate I_{HS}, we write the hot spot magnetic energy $W_{\rm magn\,HS} \equiv \int_{\rm hot\,spot} {\rm d}\mathbf{x}\, |\mathbf{B}|^2/(2\mu_0) \approx (4\pi/3) a_{HS}^3 (B_{HS}^2/2\mu_0)$ as $W_{\rm magn\,HS} = \frac{1}{2} L_{HS} I_{HS}^2$, with $L_{HS} \approx \mu_0 a_{HS}$ hot spot inductance. In summary, Ohm's law and the formula for $W_{\rm magn\,HS}$ lead to:

$$\Phi = 2 I_{HS}/(\pi \sigma_{/\!/} a_{HS}) \quad (39)$$

and to:

$$I_{HS} \approx 2(\pi/3)^{1/2} (a_{HS} B_{HS}/\mu_0) \quad (40)$$

respectively. Moreover, we write Bennett relationship for the $Z \approx 1$ hot spot:

$$16\,\pi^2\; n_{eHS}\, a_{HS}^2\; e\, T_{eHS} = \mu_0\, I_{HS}^2\, \beta_{HS}. \quad (41)$$

Together, equations (21), (32), (34), (35), (36), (38), (39), (40) and (41) are nine equations involving the ten quantities V_p, Φ, $\sigma_{/\!/}$, I_{HS}, a_{HS}, B_{HS}, n_{eHS}, T_{eHS}, n_{ec}, and T_{ec}. Then, we can write all quantities as functions of Φ, provided that the quantities $\ln\Lambda$, α and β_c/β_{HS} (which represent collisions, turbulent electron dynamics and anomalous ion viscous heating, respectively) are known.

In particular, equations (32) and (34) lead to the following useful intermediate relationship:

$$n_{eHS} a_{HS}^2 \approx 1.1 \times 10^{16}. \quad (42)$$

Then, equations (21), (34), (35), (36), (38), (39), (40), (41) and (42) give:

$$a_{HS} \approx 2.5 \xi \Phi^{-2} \quad (43)$$

where $\xi \equiv \beta_c \ln\Lambda/(\alpha\beta_{HS})$. We discuss the physical meaning of ξ in the following. In turn, equations (42) and (43) lead to:

$$n_{eHS} \approx 1.7 \times 10^{15} \xi^{-2} \Phi^4. \quad (44)$$

Moreover, equations (32), (38) and (44) give the following useful relationship:

$$T_{ec} \approx 3.3 \times 10^{-4} \xi^{1/2} n_{ec}^{1/4}. \quad (45)$$

Finally, equations (35), (38) and (45) lead to:

$$B_{HS} \approx 1.7 \times 10^{-5} \xi^{-1} \Phi^{5/2}. \quad (46)$$

Equations (43), (44) and (46) provide us with information about the hot spot at the beginning of the phase with maximum n_i, i.e. of maximum fusion rate. Further analysis requires evaluation of Φ.

To this purpose, we recall that our analysis of Poynting balance shows that Joule dissipation occurs mainly at the very end of the hot spot. Such dissipation destroys

both the magnetic helicity K and the poloidal magnetic flux Ψ, decreasing $|K|$ and $|\Psi|$ from their initial values $|K_{HS}|$ and $|\Psi_{HS}|$ to 0. The dissipation rate [60] is $dK/dt = 2\int_{\text{hot spot}} d\mathbf{x}\,\mathbf{B}\cdot\mathbf{E} \approx 2\Psi(d\Psi/dt)$, so that integration on time leads to:

$$|K_{HS}| = \int dt dK/dt = \Psi_{HS}^2. \tag{47}$$

We are going to extract information on Φ from (47). Firstly, we observe that K provides the main contribution to H in large-B, Taylor-like 3D states satisfying Turner's principle [51], i.e.

$$|K_{HS}| \approx |H_{HS}|/e^2. \tag{48}$$

Equations (4), (7), (11), (12), (14), (22), (23), (24), (33), (38), (45), (47) and (48) link Φ, Ψ_{HS}, ξ and the a_{working}'s. Straightforward algebra leads to:

$$\Psi_{HS}^2 \approx 4.5\times 10^2 \xi t_{\text{pinch}} T_{\text{working}}^{1/2} p_{\text{working}}^{1/2} W_{cb}^{5/6} a_{\text{working}}^{-1} \Phi^{-2}. \tag{49}$$

We are left with the computation of Ψ_{HS}. Under CVHBS, Ψ_{HS} and K transform just like $K^{1/2}$ and H, respectively. Then, equations (23), (24) and (33) lead to

$$\Psi_{HS} = 0.35\zeta^{-1}\Psi_{\text{pinch}} \tag{50}$$

where Ψ_{pinch} is the pinch magnetic flux and

$$\Psi_{\text{pinch}} \approx t_{\text{pinch}} V_p. \tag{51}$$

In order to derive relationship (51) we have assumed that all inductances in the PF but the pinch self-inductance are negligible. Again, this is quite optimistic assumption, but it is useful as far as we are looking for necessary conditions of ignition.

Equations (12), (22), (24), (38), (45), (49), (50) and (51) lead to:

$$\Phi = 0.3 t_{\text{pinch}}^{-1/2} a_{\text{working}}^{-1/2} T_{\text{working}}^{1/2} p_{\text{working}}^{1/4} W_{cb}^{1/3} \tag{52}$$

regardless of ξ. Equations (36), (38), (43), (44), (46) and (52) provide us with the looked-for link between the a_{HS}'s and the a_{working}'s.

8 Necessary conditions for ignition

Once applied to the a_{HS}'s, relationships (1), (2) and (3) are three necessary conditions for occurrence of ignition in the 4th phase. Substitution of equations (8), (9), (36), (43), (44), (46), (38) and (52) allow us to write such conditions in terms of the a_{working}'s, thus allowing us to assess ignition feasibility in a PF of given size, energy condenser bank, etc.

In particular, (1), (4) and (44) show that fulfilment of Lawson's criterion requires:

$$\Phi \geqslant \Phi_{\text{Lawson}}(T_{iHS}, \xi, \tau_{HS}) \equiv 1.6\times 10^{-4} f(T_{iHS}\ldots)\tau_{HS}^{-1}\xi^{1/2} \tag{53}$$

where [34] the shape of $f\,(T_{iHS}\ldots)$ for $\varepsilon = 0.09$ is roughly parabolic, with $f\,(T_{iHS} = 1.2\times 10^5) = 4.2\times 10^{21}$ and minimum at $f\,(T_{iHS} = 2.2\times 10^5) = 2.58\times 10^{21}$.

Moreover, (2) and (46) show that quantum suppression requires:

$$\Phi \geqslant \Phi_{\text{quantum}}\,(T_{iHS}, \xi) \equiv 3.9\times 10^2 T_{iHS}^{2/5}\xi^{2/5}. \tag{54}$$

This relationship holds for protons. The required B_{HS} for boron nuclei is 11 times smaller, according to (2); but there are just 9^{11}B nuclei per 100 protons, as $\varepsilon = 0.09$; focussing on protons is therefore reasonable. Furthermore, (3), (44) and (46) provide us with an upper bound on Φ:

$$\Phi_{\text{cycl}} \equiv 2.4\times 10^6 > \Phi. \tag{55}$$

Formally, equations (53)–(55) lead to the following necessary condition for ignition:

$$\Phi_{\text{cycl}} > \Phi \geqslant \Phi_{\text{treshold}}\,(T_{iHS}, \xi) \equiv \max\left(\Phi_{\text{Lawson}}, \Phi_{\text{quantum}}\right). \tag{56}$$

Now, relationships (8), (9), (52) and (56) allow us to assess if ignition is possible in a given PF, once the values of τ_{HS}, T_{iHS} and ξ are known. As far as the upper bound (55) is not violated, it turns out that strategies aiming at ignition include not just raising W_{cb}, as in mainstream PF research [3], but also raising p_{working} and lowering a_{working}; the latter choice allows, e.g. smaller hot spots to collapse to higher final densities [31,77] and – more to the point – suggests that ignition is possible even at moderate values of W_{cb}, in agreement with the claims of references [29,30]. However, it must be stressed that compatibility of these choices with the empirical scaling laws (7)–(11) listed in Section 2 remains to be assessed.

Further analysis requires estimates of both τ_{HS}, T_{iHS} and ξ or, equivalently, of energy confinement, ion and electron heating, respectively (as usual in the research on controlled nuclear fusion).

As for τ_{HS}, it is a free parameter in the following; we stick to the reasonable value $\tau_{HS} = 5$ ns, as it is easy to show that reasonable modifications of τ_{HS} leave our main conclusions unaffected below.

As for T_{iHS}, according to [34] it can be raised above 150 KeV by the mechanism outlined in reference [41]. Conservatively, we invoke here no detailed ion heating mechanism. We limit ourselves to assume that ions are heated somehow. In our search for necessary conditions of ignition, in the following we take the value $T_{iHS} = 2.2\times 10^5$ which minimises Φ_{Lawson}.

As for $\xi = \beta_c \ln\Lambda/(\alpha\beta_{HS})$, the lower its value the easier the fulfilment of (56), as both Φ_{Lawson} and Φ_{quantum} are increasing functions of ξ. Physically, the hotter the ions the larger β_{HS} and the lower ξ($\beta_c = 0.11$ is constant). Moreover, the lower $\ln\Lambda/\alpha$ the larger $\sigma_{/\!/}$ and the lower ξ. Both results are far from surprising, as we expect large Joule heating to waste energy thus preventing the hot spot from achieving ignition; in contrast, the latter requires effective ion heating. In order to estimate ξ, we still need estimates of both β_{HS}, $\ln\Lambda$ and α. As for β_{HS}, since $T_{iHS} \gg T_{eHS}$ we obtain $\beta_{HS} \approx 2\mu_0 n_{iHS} e T_{iHS} B_{HS}^{-2}$,

which according to (4), (44) and (46) reduces to:

$$\beta_{HS} \approx 2.4 T_{iHS} \Phi^{-1} \tag{57}$$

regardless of ξ. As for $\ln\Lambda$, it is strongly affected by quantum suppression [34]; since we want to check the feasibility of the scenario outlined in reference [34], we invoke their equation (9) for $\ln\Lambda$, i.e.:

$$\ln\Lambda = \ln\left(602 T_{eHS}^{1/2}\right). \tag{58}$$

As for α, we observe that the electron drift motion inside the hot spot is supersonic, i.e. $V_d > c_s$ regardless of ξ. In fact, $V_d \approx |(en_{eHS})^{-1}\mathbf{j}|$ reduces to $V_d \approx |(\mu_0 en_{eHS})^{-1} \nabla \wedge \mathbf{B}|$ for Ampère's law; in turn, equation (19) gives $V_d \approx (\mu_0 en_{eHS})^{-1} \lambda B_{HS}$ in the hot spot, and the boundary condition for a spheromak-like hot spot is $\lambda a_{HS} = 4.493$, i.e. the first zero of the first spherical Bessel function. On the other side, $c_s \approx (T_{iHS}/m_i)^{1/2}$. According to equations (43), (44) and (46), neither V_d nor c_s depend on ξ; moreover, $V_d > c_s$ even for $T_{iHS} \approx$ hundreds of KeV. Then, turbulence lowers α down to 10^{-3} at least (see both §11.1 of Ref. [1] and Ref. [72]); values of α ten times smaller are possible, but we neglect here this worst case, conservatively. Together with equations (36), (38), (57) and (58), this result gives:

$$\xi = 4.6 \times 10^1 T_{iHS}^{-1} \Phi \ln\left(225 \Phi^{1/2}\right). \tag{59}$$

In turn, relationships (8), (9), (36), (38), (52), (56) and (59) provide a constraint on W_{cb} at ignition

$$\begin{aligned} \Phi_{\rm cycl} &> \Phi(W_{cb}, t_{\rm pinch}, T_{\rm working}) \\ &\geqslant \Phi_{\rm treshold}(T_{iHS}, \xi(W_{cb}, T_{iHS})) \end{aligned} \tag{60}$$

once τ_{HS}, T_{iHS}, $T_{\rm working}$ and $t_{\rm pinch}$ are given. In particular, equations (8), (9) and (52) give $\Phi \propto W_{cb}^{1/4}$, while (59) makes $\Phi_{\rm treshold}$ to increase less than linearly with increasing Φ. Accordingly, (60) provides us with a range of values of W_{cb}; no p-^{11}B ignition is possible outside this range.

As for τ_{HS} and T_{iHS}, we have already seen that reasonable values are $\tau_{HS} = 5 \times 10^{-9}$ and $T_{iHS} = 2.2 \times 10^5$; moreover, it turns out that $\Phi_{\rm treshold} = \Phi_{\rm quantum}$ in most cases, and both τ_{HS} and T_{iHS} leave $\Phi_{\rm quantum}$ unaffected because of equation (59). As for $T_{\rm working}$, the room temperature value $T_{\rm working} = 2.5 \times 10^{-2}$ corresponds roughly to the operating condition of most experiments underlying the scaling laws in Section 2. We are just left with the dependence on $t_{\rm pinch}$.

For such values, Figure 1 displays both $\Phi_{\rm cycl}$, $\Phi_{\rm quantum}$, Φ and $\Phi_{\rm Lawson}$ as functions of W_{cb} for $t_{\rm pinch} = 2 \times 10^{-6}$ and $\alpha = 10^{-3}$. Both Lawson criterion and cyclotron screening are always satisfied, but quantum suppression occurs at no value of W_{cb}. Actually, things at $W_{cb} > 300$ kJ would be even worse, as we invoked (9) in the form valid for $W_{cb} < 300$ kJ, i.e. we included no saturation at large values of W_{cb}.

Moreover, Figure 2 displays $F \equiv \Phi/\Phi_{\rm treshold}$ as a function of $t_{\rm pinch}$ and W_{cb}. (Again, F is an increasing function of Φ because of Eq. (59).) Here and in the following, ignition is only possible if $F > 1$. It turns out that no ignition is possible in a wide range of the arguments. In agreement with (52), both increasing W_{cb} and decreasing $t_{\rm pinch}$ have a mild positive impact, as both increase Φ.

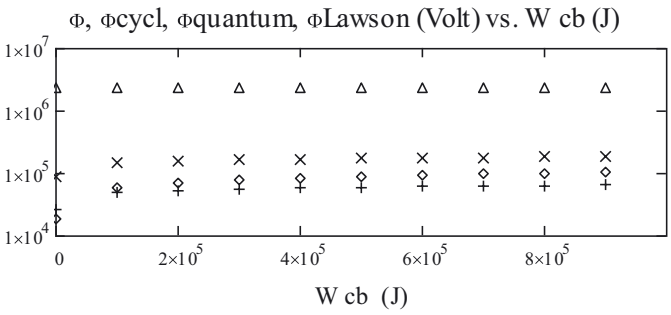

Fig. 1. Here Φ (Volt, $\diamond\diamond\diamond$), $\Phi_{\rm cycl}$ (Volt, $\Delta\Delta\Delta$), $\Phi_{\rm quantum}$ (Volt, xxx) and $\Phi_{\rm Lawson}$ (Volt, $+++$) are the potential which accelerates the electron beam emitted by the dying hot spot, the upper bound on Φ required by cyclotron radiation screening, the lower bound on Φ required by quantum suppression and the lower bound on Φ required by Lawson criterion, respectively. The energy condenser bank (Joule) is W_{cb}. Here $\alpha = 10^{-3}$ (turbulence-enhanced resistivity) and the filamentary current sheath travels down to the end of the anode in a time $t_{\rm pinch} = 2 \times 10^{-6}$ s. No ignition is possible as $\Phi_{\rm quantum} > \Phi$ (i.e., no quantum suppression may occur) in the range $0 \leqslant W_{cb} \leqslant 1$ MJ.

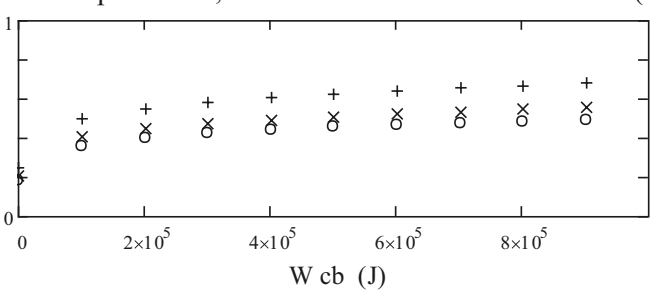

Fig. 2. $F \equiv \Phi/\max(\Phi_{\rm Lawson}, \Phi_{\rm quantum})$ (dimensionless) vs. $W_{cb}(J)$ for $\alpha = 10^{-3}$ and $t_{\rm pinch} = 10^{-6}$ s (continuous line), $t_{\rm pinch} = 2 \times 10^{-6}$ s (xxx) and $t_{\rm pinch} = 3 \times 10^{-6}$ s (ooo). Ignition is only possible for $F > 1$.

Among all phenomena which prevent ignition, it turn out that by far the most relevant is turbulence, i.e. α. Should no turbulence occur (i.e. $\alpha = 1$), $\sigma_{/\!/}$ would be equal to its Spitzer value in equation (21). In this case, Figure 3 shows that ignition would be possible at all values of W_{cb}. Such conclusion is so optimistic that it makes our estimate $\alpha \ll 1$ to be a reasonable one.

9 Possible refinements

9.1 Generalities

At a first glance our arguments leave no room to ignition. Admittedly, however, the weak point in our discussion is that our starting point, the empirical scaling laws

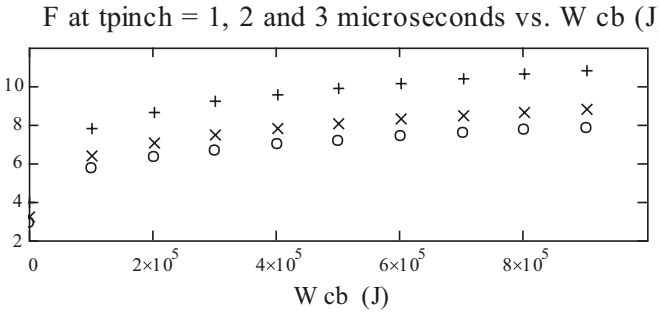

Fig. 3. F (dimensionless) vs. $W_{cb}(J)$ for $\alpha = 1$ (i.e. no turbulence: Spitzer law holds for $\sigma_{/\!/}$) and $t_{\rm pinch} = 10^{-6}$ s (continuous line), $t_{\rm pinch} = 2 \times 10^{-6}$ s (xxx) and $t_{\rm pinch} = 3 \times 10^{-6}$ s (ooo). $F > 1$ (hence, ignition is possible) at all values of W_{cb} in the range $0 \leqslant W_{cb} \leqslant 1$ MJ.

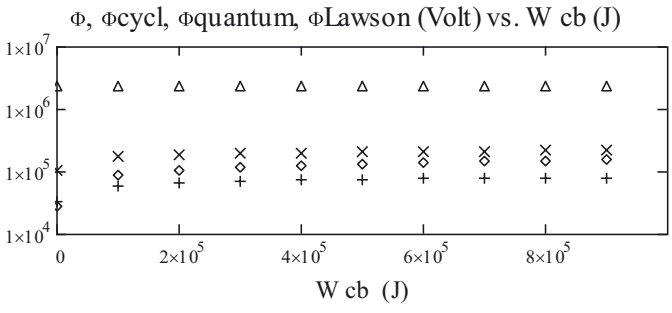

Fig. 4. Φ (Volt, $\diamondsuit\diamondsuit\diamondsuit$), $\Phi_{\rm cycl}$ (Volt, $\Delta\Delta\Delta$), $\Phi_{\rm quantum}$ (Volt, xxx) and $\Phi_{\rm Lawson}$ (Volt, $+++$) vs. $W_{cb}(J)$. Here, $\alpha = 10^{-3}$, $t_{\rm pinch} = 2 \times 10^{-6}$ s, $u = 1$ (maximum injection of angular momentum) and $R = 0$ (no back-reflection of Bremsstrahlung). No ignition is possible as $\Phi_{\rm quantum} > \Phi$ (i.e., no quantum suppression may occur) in the range $0 \leqslant W_{cb} \leqslant 1$ MJ.

of Section 2, are just rule-of-thumb descriptions, where considerable uncertainty affects the values of numerical constants. This fact weakens the robustness of our pessimistic conclusion in Section 8. Furthermore, it can be argued that they do not take into account the favourable impact of dust [81] and of field distortion elements [26]. Moreover, equation (52) seems to confirm the strategy of reference [30] aiming at reducing $a_{\rm working}$ and raising $p_{\rm working}$. Finally, our scaling laws take into account no injection of angular momentum [30] and no back-reflection of Bremsstrahlung [86]. Both these techniques seem to play a beneficial role. Accordingly, we try to provide some insight on the impact of such techniques on the feasibility of p-^{11}B ignition in the following.

9.2 Injection of angular momentum

Crudely speaking, we expect the injection of angular momentum (no matter how accomplished in practice) to facilitate ignition. In fact, the larger the angular momentum $L_{\rm pinch}$, the larger the azimuthal contribution $W_{az} \equiv \int_{\rm pinch} d\mathbf{x}\, \frac{\rho\,|v_\theta|^2}{2} = L^2_{\rm pinch}/(2\rho a^3_{\rm working}) \geqslant 0$ to $W_{\rm kin\,pinch}$, where v_θ is the azimuthal component of $\mathbf{v}$ and $\rho a^3_{\rm working} \approx$ the total mass of the plasma. In turn, the larger W_{az} the larger $|\nabla \mathbf{v}|$, as symmetry requires $v_\theta = 0$ on the PF symmetry axis. Moreover, the larger $|\nabla \mathbf{v}|$ the larger the amount $\propto |\nabla \mathbf{v}|^2$ of power dissipated by viscosity. Finally, the larger such amount, the more effective the (viscosity-driven) ion heating, the larger E_{iHS}, the easier the quantum suppression in equation (2) (Our argument needs no Maxwellian ions.) All the way around, given T_{iHS} and W_{cb} we expect F to be an increasing function of $L_{\rm pinch}$.

Of course, $L_{\rm pinch}$ cannot be arbitrarily large. When the centrifugal force exceeds the magnetic pinch force, it destroys the pinch. We require therefore that $W_{az} \leqslant W_{\rm magn\,pinch} \equiv \int_{\rm pinch} d\mathbf{x}\ |\mathbf{B}|^2/(2\mu_0)$. The latter quantity obeys the following scaling law [53]:

$$W_{\rm magn\,pinch} \approx 0.74 W_{cb}. \quad (61)$$

More rigorously, we recall that our scaling laws in Section 2 have been derived from experiments with no injection of angular momentum: we write therefore $W_{az} = 0$ for such experiments, for simplicity. (This is reasonable, as the impact on kinetic energy of any possible amount of angular momentum contained in the pinch before injection is already taken into account in $W_{\rm kin\,pinch}$.) The easiest way to take into account this injection while preserving the physical meaning of the scaling laws is to replace $W_{\rm kin\,pinch}$ with $W_{\rm kin\,pinch} + W_{az}$ everywhere. According to (11) and (61), this is equivalent to replace W_{cb} with $W_{cb}(1 + 4.4u)$ in (60), where $0 \leqslant u \leqslant 1$; $u = 0$ and $u = 1$ correspond to minimum (zero) and maximum injection of angular momentum, as allowed by centrifugal force.

9.3 Back-reflection of Bremsstrahlung

In all cases considered so far with turbulent, $\alpha = 10^{-3}$ plasmas, it is the lack of quantum suppression which makes ignition impossible. Implicitly, however, we have assumed that all the radiative power emitted through Bremsstrahlung by the plasma is lost. Obviously, if a fraction at least of this Bremsstrahlung power is reflected somehow [87] back to the plasma, then ignition becomes easier [86]. In order to discuss this point, we proceed as follows. Of course, should no Bremsstrahlung exist, $\Phi_{\rm quantum}$ would vanish. Accordingly, we denote the fraction of reflected Bremsstrahlung with R, where $0 \leqslant R \leqslant 1$; moreover, we replace $\Phi_{\rm quantum}(T_{iHS}, \xi)$ by $(1 - R)\Phi_{\rm quantum}(T_{iHS}, \xi)$ in (60). The latter criterion becomes therefore:

$$\Phi_{\rm cycl} > \Phi(W_{cb}(1 + 4.4u),\ t_{\rm pinch},\ T_{\rm working}) \geqslant \Phi_{\rm treshold}(T_{iHS},\ \xi(W_{cb}(1 + 4.4u),\ T_{iHS}),\ R). \quad (62)$$

9.4 Results

Figures 1 and 2 display the results for $u = 0$ (no injected angular momentum) and $R = 0$ (no reflection of Bremsstrahlung). Figures 4 and 5 display the corresponding results for maximum injection ($u = 1$) and $R = 0$

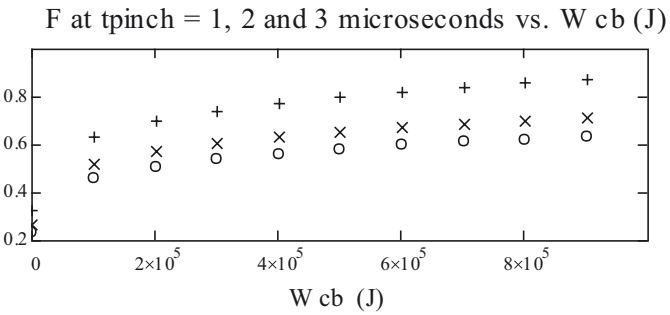

Fig. 5. F vs. $W_{cb}(J)$ for $\alpha = 10^{-3}$ and $t_{\text{pinch}} = 10^{-6}$ s (+++), $t_{\text{pinch}} = 2 \times 10^{-6}$ s (xxx) and $t_{\text{pinch}} = 3 \times 10^{-6}$ s (ooo); $u = 1$ (maximum injection of angular momentum), $R = 0$ (no back-reflection of Bremsstrahlung). Ignition is only possible for $F > 1$.

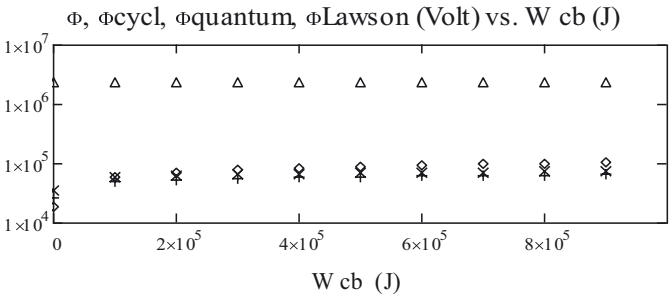

Fig. 6. Φ (Volt, $\Diamond\Diamond\Diamond$), Φ_{cycl} (Volt, $\Delta\Delta\Delta$), Φ_{quantum} (Volt, xxx) and Φ_{Lawson} (Volt, + + +) vs. $W_{cb}(J)$. Here, $\alpha = 10^{-3}$, $t_{\text{pinch}} = 2 \times 10^{-6}$ s, $u = 0$ (no injection of angular momentum), $R = 0.6$ (i.e., 60% of Bremsstrahlung power is reflected back). If W_{cb} is large enough, then all necessary conditions for ignition ($\Phi_{\text{cycl}} > \Phi > \Phi_{\text{quantum}}$, Φ_{Lawson}) are satisfied simultaneously, i.e. ignition becomes possible.

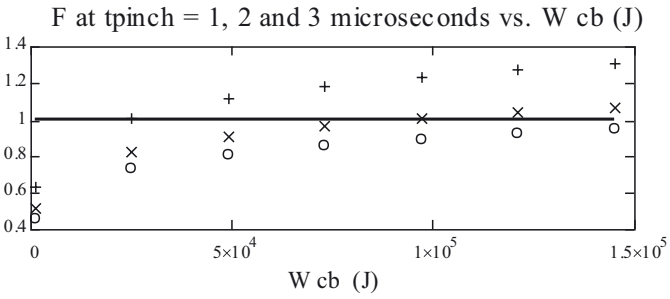

Fig. 7. F vs. W_{cb} for $\alpha = 10^{-3}$ and $t_{\text{pinch}} = 10^{-6}$ (+ + +), $t_{\text{pinch}} = 2 \times 10^{-6}$ (xxx) and $t_{\text{pinch}} = 3 \times 10^{-6}$ (ooo); $\alpha = 10^{-3}$; $u = 0$ (no injection of angular momentum), $R = 0.6$ (i.e., 60% of Bremsstrahlung power is reflected back). The bold straight horizontal line is $F = 1$. Ignition is only possible for $F > 1$.

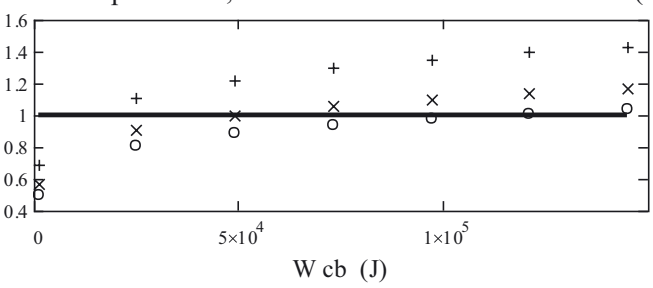

Fig. 8. F vs. W_{cb} for $\alpha = 10^{-3}$ and $t_{\text{pinch}} = 10^{-6}$ (+ + +), $t_{\text{pinch}} = 2 \times 10^{-6}$ (xxx) and $t_{\text{pinch}} = 3 \times 10^{-6}$ (ooo); $\alpha = 10^{-3}$; $u = 0.2$ (i.e. 20% of maximum allowable angular momentum is injected); $R = 0.6$ (i.e., 60% of Bremsstrahlung power is reflected back). The bold straight horizontal line is $F = 1$. Ignition is only possible for $F > 1$.

(no reflection). Even in this case, no ignition seems to be possible.

Even if no angular momentum is injected ($u = 0$), it turns out that ignition becomes possible at $W_{cb} \approx 150$ kJ if 60% of Bremsstrahlung power is reflected back ($R = 0.6$). This result agrees with figure 3 of reference [86], which we take as independent confirmation of our result. Figures 6 and 7 display the same results of Figures 1 and 2 for $u = 0$, $R = 0.6$. Reasonably, such a low value of the reflection coefficient R is likely to allow utilisation of mirrors with relatively broad band [87].

Finally, simultaneous injection of angular momentum and Bremsstrahlung reflection makes things easier, i.e. lowers the required value for W_{cb} at all values of t_{pinch} or, equivalently, reduces the required R at given W_{cb}. Figure 8 displays results for the case $u = 0.2$, $R = 0.6$.

10 Conclusions

The Plasma Focus (PF) is a cheap, source of pulsed, extremely dense plasmas at temperatures > KeV, whose power supply is provided by a condenser bank with energy W_{cb} [1]. When operating in deuterium, the observed yield Y_n of DD fusion neutron per shot scales approximately as $Y_n \propto W_{cb}^2$. Such favourable scaling made the PF the natural candidate for controlled nuclear fusion, until the saturation of $Y_n(W_{cb})$ observed at $W_{cb} \approx 300$ kJ, far below DD ignition, led to suppression of most PF-related fusion research [2].

Through a succession of instabilities, PF discharges evolve spontaneously towards configurations of ever increasing particle density. Small, short-lived regions ("hot spots") of exceedingly large electron density are routinely observed in the final phase of PF discharges. Some experiments suggest that both the absolute value B of the magnetic field, the ion temperature and the electron density n_e may attain record values in a hot spot, so that the ion thermal energy may become ≈ the energy gap between adjacent electronic Landau levels in future experiments. To date, ion energies above 150 KeV have been reported [31], which recall similar results in Z-pinches [41]. Should this prediction be confirmed, then collisional energy transfer from ions and electrons would strongly decrease ("quantum suppression"). In turn, such suppression would reduce Bremsstrahlung losses significantly in a suitable hydrogen-boron plasma. Moreover, large values of n_e

would provide effective screening of cyclotron radiation, with further reduction of energy losses. In this case, ion heating would allow the hot spot to fulfil Lawson criterion, and the hot spot could attain p-^{11}B ignition even at moderate W_{cb}. Controlled, aneutronic nuclear fusion would therefore be at hand.

Recently, US and Iranian researchers [22,28–30,34] undertook both an experimental campaign and numerical simulations, aiming at p-^{11}B ignition according to the suggestions listed above. They claim that ignition is possible even at $W_{cb} < 300$ kJ, provided that the working pressure (the anode radius) is slightly larger (smaller) than the value predicted by the empirical scaling laws [2] ruling PFs tuned for optimal operation. In this scenario PF evolution is a multi-step process, leading to a final configuration with maximum particle density where quantum suppression occurs and Lawson criterion is satisfied. Since the rate of fusion reactions is an increasing function of particle density, this final configuration may be of interest to ignition. Ion heating is provided by the mechanism described in reference [41]; Joule heating is not taken into account explicitly.

In the present work we aim at checking the self-consistency of the scenario outlined above. To this purpose, we invoke both well-known scaling-laws [2] and – in order to take Joule heating properly into account – the scaling invariance of the collisional kinetic equations, a property usually invoked in controlled fusion research [71]. Once we take the occurrence of the multi-step evolution towards high-density states as granted, these scaling properties link the values of physical quantities like magnetic field, electron density, etc. at the end of each step to the initial conditions of the discharge (W_{cb}, the working pressure, etc.). If ignition is to occur in the final, high-density state, then the simultaneous occurrence of quantum suppression, cyclotron screening and fulfilment of Lawson criterion provide a necessary condition for ignition, to be satisfied at the end of the discharge. Then, the above discussed link of the final and the initial conditions provide us with a constraint (our relationship (62)) to be satisfied by the initial conditions of a PF discharge aiming at ignition.

Unlike [30,34], our discussion depends on no detailed mechanism of ion heating. Moreover, Poynting balance of electromagnetic energy shows that the impact of Joule heating on energy balance is relevant in the very final stage of the discharge only. All the same, Joule heating still rules a crucial role in the (usually overlooked) evolution of generalised helicity as the plasma evolves; we show that the evolution of the plasma is a succession of relaxed configurations (two-dimensional filaments, three-dimensional, spheromak-like hot spots) known in the literature as double Beltrami states. The latter have been investigated in astrophysics [84], just like quantum suppression itself [43]. This link of PF physics with astrophysics confirms old suggestions [15].

Since we are looking for a necessary condition, we are allowed to invoke very optimistic assumptions: violation of the condition even under optimistic assumption prevents the PF from attaining ignition a fortiori. Here, we refer to the assumptions leading to our equations (32), (38), (51) and (59): they correspond to the choice of the highest value allowed of n_e in the hot spot, the identification of the accelerating electric voltage across one hot spot with the corresponding voltage across the plasma, negligible inductances in the PF (but the pinch self-inductance itself), and a rather mild level of turbulence (which enhances the electrical resistivity just by a factor 10^3 above its Spitzer value) respectively. Finally, no saturation at large values of W_{cb} has been considered.

It turns out that – *as far as the empirical scaling laws quoted above hold* – the necessary condition (60) for p-^{11}B ignition is satisfied at no value of $W_{cb} < 1$ MJ, for various values of the discharge life-time, hot-spot life-time, etc. The trouble is that if any physical mechanism, no matter what its nature is like, raises particle density towards fusion-relevant values, then the scaling invariance of kinetic equations requires that also the density of electromagnetic energy increases by orders of magnitude. The corresponding amplitude of the electric field becomes therefore very large, leading to acceleration of electrons up to supersonic velocities. This triggers turbulence, which in turn raises the electric resistivity and, as a consequence, the Joule heating. The latter transforms irreversibly into heat the energy that would otherwise be available for further compression, thus preventing further increase of particle density. The analysis of references [28,30,34] overlooks this fact because it focuses on ion heating and the collisional exchange of energy between ions and electrons, while neglecting proper treatment of Joule heating of electrons. (Should we able to suppress turbulence altogether, ignition would be possible at all values of W_{cb}. Reference [28] even invokes the scaling law $B/n_e = $ const. of ideal magnetohydrodynamics.)

Admittedly, the relevance of available scaling laws to our problem is questionable, to say the least. First of all, they are just rule-of-thumb descriptions, affected by considerable incertitude as far as we are concerned about numerical estimates. Secondly, they have been obtained for PF with optimum yield of DD neutrons and X-rays, while here we are dealing with p-^{11}B plasmas. Thirdly, they describe no experiment with either addition of dust on PF pinch axis [81], inclusion of "field distortion elements" [26] or injection of angular momentum [30], which seem to affect plasma performances positively. Furthermore, values of initial working pressure (anode radius) slightly larger (smaller) than predicted by these scaling laws also seem to play a favourable role. Finally, to date no attempt has even been made – to the author's knowledge – in order to reflect a fraction of the power lost through Bremsstrahlung back to the plasma [86]. Our analysis shows that, even if injection of angular momentum per se is not enough to allow ignition, a 60% reflection of Bremsstrahlung would do the job even at $W_{cb} \approx 150$ kJ, i.e. far below the saturation at $W_{cb} \approx 300$ kJ, with no injection of angular momentum. Simultaneous injection of angular momentum and reflection of Bremsstrahlung radiation seems to make ignition even easier. Moreover, it is conceivable that the lower the

required reflection coefficient, the broader the band of the mirrors to be utilised [87].

In conclusion, we stress that we have just dealt with necessary conditions for p-^{11}B ignition. Possibility does not imply reality. For example, independent confirmation of the huge ion energies reported in reference [31] is required. In our opinion, however, systematic investigation of the matter definitely deserves further attention.

Useful discussions with Prof. R. Miklaszewski of IFPILM, Warsaw and F. Fontana, Micos Engineering GmbH, Zuerich on scaling laws and mirrors respectively are gratefully acknowledged.

Appendix

Proof of (14)

Approximately, we write

$$H_{\rm pinch} \approx \left(\frac{dH}{dt}\right) t_{\rm pinch} + H_{\rm working}.$$

The linear size of the PF discharge chamber is much larger than the collisionless ion depth (ω_{pi} ion plasma frequency); it follows that [51]

$$H \approx m_i^2 \int d\mathbf{x}\ \mathbf{v}\cdot\omega \quad \text{where} \quad \omega = \nabla\times\mathbf{v}.$$

Ions are initially at rest, so $H_{\rm working} = 0$. Since the PF volume is constant,

$$\frac{dH}{dt} = \frac{\partial H}{\partial t} \approx m_i^2 \frac{\partial}{\partial t}\left(\int d\mathbf{x}\ \mathbf{v}\cdot\omega\right).$$

After repeated integration by parts, equation (13) leads to

$$\frac{\partial}{\partial t}\left(\int d\mathbf{x}\ \mathbf{v}\cdot\omega\right) = 2\int d\mathbf{x}\ \mathbf{v}\cdot\nabla\wedge\left(\frac{\mathbf{j}\wedge\mathbf{B}}{\rho}\right) + \int d\mathbf{x}\ p\ \omega\cdot\nabla\left(\frac{1}{\rho}\right).$$

Now, we recall that the PF plasma sheath pushes ahead the working gas in its movement towards the hollow end of the anode, so that $\nabla\rho$ is everywhere orthogonal to the sheath. Moreover, the sheath is made of many tiny, helicoidal filaments [4], each of them with its own ω tangent to the sheath. It follows that $\omega\cdot\nabla\left(\frac{1}{\rho}\right) = 0$. Moreover, $\mathbf{j}\neq 0$ in filaments only; we apply equation (8.2) of reference [48] to each filament and obtain $\mathbf{j}/\rho = e\mathbf{v}/m_e$, so that

$$\frac{\partial}{\partial t}\left(\int d\mathbf{x}\ \mathbf{v}\cdot\omega\right) = \frac{2\,e}{m_e}\int d\mathbf{x}\ \left[\mathbf{v}\cdot(\mathbf{B}\cdot\nabla)\ \mathbf{v} - (\mathbf{v}\cdot\mathbf{B})\ (\nabla\cdot\mathbf{v}) - \mathbf{v}\cdot(\mathbf{v}\cdot\nabla)\ \mathbf{B}\right]$$

as $\nabla\cdot\mathbf{B} = 0$ for Gauss' law. The volume integral is performed on the whole PF chamber, so that the non-zero contributions are due to the azimuthal field $\mathbf{B} = B_\theta\boldsymbol{\theta}$, where $B_\theta = B_\theta(r,t) = \mu_0 I(t)/(2\pi r)$, and I, r and $\boldsymbol{\theta}$ are the current, the radial coordinate and the unit vector in the azimuthal direction respectively. Azimuthal symmetry implies that the contribution of $(\mathbf{B}\cdot\nabla)\ \mathbf{v} \propto \partial\mathbf{v}/\partial\theta$ is negligible. As for the remaining terms, the largest contribution comes from the instants just before the radial implosion of the filaments towards the PF axis, as $|\mathbf{B}|$ increases with increasing I and decreasing r. In this phase $\mathbf{v}$ is mainly radial; as a consequence, we are allowed to write: $\mathbf{v}\cdot\mathbf{B}\approx 0$. We are left with

$$\begin{aligned}\frac{\partial}{\partial t}\left(\int d\mathbf{x}\ \mathbf{v}\cdot\omega\right) &= -\frac{2\,e}{m_e}\int d\mathbf{x}\ \mathbf{v}\cdot(\mathbf{v}\cdot\nabla)\ \mathbf{B}\\ &= \frac{\mu_0\, e\ I(t)}{\pi\, m_e}\int d\mathbf{x}\ \frac{|\mathbf{v}|^2}{r^2}\\ &\approx \frac{2\ \mu_0\, e\ I_{\rm pinch} W_{\rm kin\ pinch}}{\pi\, n_{i\ \rm pinch} m_i m_e a^2_{\rm working}},\end{aligned}$$

where we have taken into account that $\rho \approx n_i m_i$. Together, the above relationships lead to equation (14).

References

1. A. Bernard, H. Bruzzone, P. Choi, H. Chuaqui, V. Gribkov, J. Herrera, K. Hirano, A. Krejčí, S. Lee, C. Luo, F. Mezzetti, M. Sadowski, H. Schmidt, K. Ware, C.S. Wong, W. Zoita, J. Moscow Phys. Soc. **8**, 93 (1998)
2. L. Soto, Plasma Phys. Control. Fusion **47**, A361 (2005)
3. J.P. Rager, in *Unconventional Approaches to Fusion*, edited by B. Brunelli, G. Leotta (Plenum Press, New York, 1982)
4. A. Di Vita, J. Plasma Phys. **50**, 1 (1993)
5. S. Lee, Appl. Phys. Lett. **95**, 151503 (2009)
6. H. Herold, A. Jerzykiewicz, M. Sadowski, H. Schmidt, Nucl. Fusion **29**, 1255 (1989)
7. M. Sadowski, H. Herold, H. Schmidt, M. Shakatre, Phys. Lett. A **105**, 117 (1984)
8. G.J. Morales, J.E. Maggs, A.T. Burke, J.R. Penano, Plasma Phys. Control. Fusion **41**, A519 (1999)
9. S. Cable, T. Tajima, Phys. Rev. A **46**, 3413 (1992)
10. J.W. Mather, Phys. Fluids **8**, 366 (1965)
11. L. Jakubowski, M.J. Sadowski, Braz. J. Phys. **32**, 1871 (2002)
12. W.H. Bostick, V. Nardi, W.J. Prior, J. Plasma Phys. **8**, 7 (1972)
13. K.N. Koshelev, V.I. Krauz, N.G. Reshetnyak, R.G. Saluvadze, Y.V. Sidel'nikov, E.Y. Khautiev, J. Phys. D **21**, 1827 (1988)
14. J.M. Byaley, G. Decker, W. Kies, M. Maelzig, F. Mueller, P. Roewekamp, J. Westheide, Y.V. Sidel'nikov, J. Appl. Phys. **69**, 613 (1991)
15. W. Bostick, Int. J. Fusion Energy **3**, 68 (1985)
16. W.H. Bostick, V. Nardi, W.J. Prior, F. Rodriguez-Trelles, in *Proceeding 2nd Intl. Conf. Pulsed & High Beta Plasmas, Garching, Germany, 1972*
17. F. Casanova, A. Tarifeño-Saldivia, F. Veloso, C. Pavez, A. Clausse, L. Soto, J. Fusion Energy **31**, 3 (2012)

18. E. Angeli, A. Tartari, M. Frignani, V. Molinari, D. Mostacci, F. Rocchi, M. Sumini, Nucl. Technol. Radiat. Protect. **20**, 33 (2005), ntrp.vin.bg.ac.yu/2005_1/1_2005Angeli_p33_37.pdf
19. V. Nardi, in *Proceeding 2nd Intl. Conf. Pulsed High Beta Plasmas, Garching, Germany, 1972*
20. J.J.E. Herrera, F. Castillo, *On The Magnetohydrodynamic Evolution Of The $m = 0$ Instability In The Dense Z-Pinch* (1998), http://epsppd.epfl.ch/Praha/WEB/98ICPP_W/L003PR.PDF
21. R.K. Rout, A. Shyam, Pramana J. Phys. **37**, 93 (1991)
22. H.R. Yousefi, T. Haruki, J.I. Sakai, A. Lumanta, K. Masugata, Phys. Lett. A **373**, 27 (2009)
23. W.H. Bostick, V. Nardi, W.J. Prior, R. Trelles, in *Proceeding 4th Conf. Contr. Fusion Plasma Phys. Grenoble, France, 1972* (Commissariat à l'Énergie atomique, 1972), Vol. 1, p. 70
24. J.S. Brzosko et al., Nuclear Reactivity In Submillimetric Domains Of Focussed Discharges, in *16th EPS, Venezia, Italy, 1989*
25. E.Yu. Khautiev, V.I. Krauz, N.G. Reshetnyak, R.G. Salukvadze, A.A. Batenyuk, A.Ch. Chkhaidze, K.N. Koshelev, Yu.V. Sidelnikov, V.A. Gribkov, O.N. Krokhin, in *Plasma Physics and Controlled Nuclear Fusion Research 1988* (International Atomic Energy Agency, Vienna, 1989), Vol. 2, pp. 579–586, http://www-naweb.iaea.org/napc/physics/FEC/STIPUB787_VOL2.pdf
26. V. Nardi, L. Bilbao, A. Bortolotti, J.S. Brzosko, C. Powell, D. Zeng, in *Plasma Physics and Controlled Nuclear Fusion Research 1988* (International Atomic Energy Agency, Vienna, 1989), Vol. 2, pp. 743–750, http://www-naweb.iaea.org/napc/physics/FEC/STIPUB787_VOL2.pdf
27. *Plasma Focus Apparatus With Field Distortion Elements*, European Patent Office Patent No. EP0312587B1
28. E.J. Lerner, Laser Particle Beams **4**, 193 (1986)
29. E.J. Lerner, in *Conf. Current Trends in International Fusion Research, Washington, USA, 2003*
30. E.J. Lerner, S.K. Murali, A. Haboub, J. Fusion Energy **30**, 367 (2011)
31. E.J. Lerner, S.K. Murali, D. Shannon, A.M. Blake, F. Van Roessel, Phys. Plasmas **19**, 032704 (2012)
32. S. Son, *Reaction rates and other processes in dense plasma* UMI Number: 3180070 (2005)
33. J.M. Martinez-Val et al., Phys. Lett. A **216**, 142 (1996)
34. S. Abolhasani, M. Habibi, R. Amrollahi, J. Fusion Energy **32**, 189 (2012)
35. S. Stave, M.W. Ahmed, R.H. France III, S.S. Henshaw, B. Muller, B.A. Perdue, R.M. Prior, M.C. Spraker, H.R. Weller, Phys. Lett. B **696**, 26 (2011)
36. National Nuclear Data Center Web Site, http://www.nndc.bnl.gov/
37. W.L. Harries, J.H. Lee, Plasma Phys. **20**, 95 (1978)
38. F. Castillo-Mejía, M. Milanese, M. Moroso, J. Pouzo, M. Santiago, in *Proceeding Intl. Conf. Plasma Physics, European Physical Society, Praha, Czech Republic, 1998*
39. N.K. Neog, S.R. Mohanty, E. Hotta, J. Appl. Phys. **99**, 013302 (2006)
40. Y. Ono, M. Yamada, T. Akao, T. Tajima, R. Matsumoto, Phys. Rev. Lett. **76**, 3328 (1996)
41. M.G. Haines, P.D. LePell, C.A. Coverdale, B. Jones, C. Deeney, J.P. Apruzese, Phys. Rev. Lett. **96**, 075003 (2006)
42. S. Son, N.J. Fisch, Phys. Lett. A **356**, 65 (2006)
43. J.R. McNally, Nucl. Fusion **15**, 344 (1975)
44. G.S. Miller, E.E. Salpeter, I. Wassermann, Astrophys. J. **314**, 215 (1987)
45. U. Das, B. Mukhopadyay, Phys. Rev. Lett. **110**, 071102 (2013)
46. S. Son, N.J. Fisch, Phys. Lett. A **329**, 76 (2004)
47. M. Halper, *Iranian Team To Collaborate With US Company On Nuclear Fusion Project*, The Guardian, 25th May 2012, http://www.guardian.co.uk/environment/2012/may/25/iranian-team-collaborate-us-nuclear
48. A. Di Vita, Eur. Phys. J. D **54**, 451 (2009)
49. D. Butler, Nature **480**, 19 (2011)
50. D. Clery, Science **337**, 1444 (2012)
51. L. Turner, IEEE Trans. Plasma Sci. **14**, 849 (1986)
52. S. Lee, Radiation Enhancement And Applications - Scaling From The UNU/ICTP PF, Invited Paper, in *International Meeting on Frontiers of physics, Satellite Meeting: 12 Years of UNU/ICTP PFF - A Review, 1998, Kuala Lumpur* (International Centre for Theoretical Physics, Italy), pre-print 33–46, http://www.plasmafocus.net/IPFS/otherpapers/RadEnhancels98.pdf
53. Th.J. Dolan, *Fusion Research* (Pergamon, New York, 1980)
54. S. Lee, in *Proceedings 1st Cairo Conf. Plasma Physics & Applications, Cairo, Egypt, 2003*, edited by H.J. Kunze, T. El-Khalafawy, H. Hegazy, volume 34 of International Cooperation Bilateral Seminars (Bilateral Seminars of the International Bureau, Forschungszentrum Jülich GmbH), pp. 27–33, http://www.plasmafocus.net/IPFS/otherpapers/charactPfSpeedEnhanceCairo03.pdf
55. J.A. Shercliff, *A Textbook of Magnetohydrodynamics* (Pergamon, New York, 1965)
56. A. Sestero, B.V. Robouch, S. Podda, Plasma Phys. **22**, 1039 (1990)
57. R. Deutsch, W. Grauf, H. Herold, H. Schmidt, Plasma Phys. **25**, 833 (1983)
58. H.A.B. Bodin, Nucl. Energy **29**, 57 (1990)
59. H. Lamb, *Hydrodynamics* (Cambridge University Press, Cambridge, 1906)
60. A.H. Boozer, Phys. Fluids B **4**, 2845 (1992)
61. E.T. Jaynes, Annu. Rev. Phys. Chem. **31**, 579 (1980)
62. F. Herrmann, Eur. J. Phys. **7**, 130 (1986)
63. L.D. Landau, E. Lifshitz, *Electrodynamics of Continuous Media* (Pergamon, New York, 1960)
64. J.B. Taylor, Phys. Rev. Lett. **33**, 1139 (1974)
65. M.R. Brown, J. Plasma Phys. **57**, 203 (1997)
66. P.M. Bellan, *Spheromaks* (Imperial College Press, London, 2000)
67. J.B. Taylor, Commun. Plasma Phys. **14**, 127 (1991)
68. Z. Yoshida, S.M. Mahajan, Phys. Rev. Lett. **88**, 095001 (2002)
69. S.K.H. Auluck, Phys. Plasmas **18**, 032508 (2011)
70. M.S. Janaki, B. Dasgupta, Phys. Plasmas **19**, 032113 (2012)
71. J.W. Connor, J.B. Taylor, Nucl. Fusion **17**, 1047 (1977)
72. H. Krompholz, G. Herziger, in *Chaos and Order in Nature*, edited by H. Haken (Springer-Verlag, Berlin, 1981)
73. G.A. Navratil, in *43rd American Physical Society Division of Plasma Physics Meeting, Long Beach, CA, USA, 2001*, http://fire.pppl.gov/apsdpptutorialrgon.pdf
74. http://www.lawrencevilleplasmaphysics.com/images/Japan%20Collaboration%20Announcement.pdf
75. V.V. Vikhrev et al., Sov. J. Plasma Phys. **8**, 688 (1982)

76. P. Antsiferov, D. Franz, R. Pfau, A. Rupasov, H. Schmidt, D. Schulz, in *Proceeding 2nd Intl. Conf. High-Beta Plasmas, Garching, Germany, 1972*
77. S. Goudarzi, A. Raeisdana, J. Fusion Energy **29**, 103 (2010)
78. A. Di Vita, Eur. Phys. J. D **56**, 205 (2010)
79. N. Ryusuke, Y. Zensho, H. Takaya, J. Plasma Fusion Res. Ser. **6**, 130 (2004)
80. S.M. Mahajan, S. Yoshida, Phys. Rev. Lett. **81**, 4863 (1998)
81. V.I. Krauz, Phys. Control. Fusion **48**, B221 (2006)
82. M. Iqbal, P.K. Shukla, Phys. Plasmas **19**, 033517 (2012)
83. D. Kagan, S.M. Mahajan, Mon. Not. R. Astron. Soc. **406**, 1140 (2010)
84. S. Ohsaki, N.L. Shatashvili, Z. Yoshida, S.M. Mahajan, ApJ **559**, L61 (2001)
85. L. Jakubowski, M. Sadowski, in *Proceeding 26th EPS Conf. Contr. Fus. Plasma Phys., Maastricht, The Netherlands, 1999*
86. R. Thomas, Y. Yang, G.H. Miley, F.B. Mead, AIP Conf. Proc. **746**, 536 (2005)
87. K.D. Joensen, P. Gorenstein, P. Høghøj, J. Susini, F. Christensen, J. Wood, G. Gutman, E. Ziegler, A. Freund, Nucl. Instrum. Methods Phys. Res. B **132**, 221 (1997)